U.S. Department of the Interior
U.S. Geological Survey

Acid-rock drainage at Skytop, Centre County, Pennsylvania, 2004

by

Jane M. Hammarstrom[1], Keith Brady[2], and Charles A. Cravotta III[3]

Open-File Report 2005-1148

[1] U.S. Geological Survey, 954 National Center, Reston, VA 20192 jhammars@usgs.gov
[2] PA Department of Environmental Protection, PO Box 8461, Harrisburg, PA 17105
[3] U.S. Geological Survey, 215 Limekiln Road, New Cumberland, PA 17070

Preface

Construction along Interstate Highway 99 during 2003 exposed sulfidic rock within a fresh roadcut on Bald Eagle Mountain at Skytop, near State College, in Centre County, central Pennsylvania. The cut exposed pyrite veins associated with an unmined, sandstone-hosted, zinc-lead deposit. Excavated rock was crushed and used locally as road base and fill. Within months, acidic (pH<3), metal-laden seeps and surface runoff from the crushed rock piles and roadcut raised concerns about surface- and ground-water contamination and prompted a halt in road construction and the beginning of costly remediation.

The Pennsylvania Department of Transportation (PennDOT) and the Pennsylvania Department of Environmental Protection expanded their site investigations and monitoring in response to the acid-drainage problem to determine the extent of the environmental effects at Skytop and to develop long-term remediation strategies. In addition, those agencies sought information on the source of the acid drainage and on the processes that led to the formation of acid-rock drainage at Skytop to assist them in selecting appropriate remediation for Skytop and in avoiding similar problems in other areas. A conference on "Principles of Acid Pollution Control Along Highways" was convened by the Department of Geosciences of the Pennsylvania State University and the ClearWater Conservancy in December of 2004 to facilitate information exchange between scientists, engineers, environmental professionals, and the public. The conference highlighted a number of ongoing topical studies (geology, structure, conditions of formation of the mineral deposit, nature of the acid drainage problem, potential treatments) that are underway at the Pennsylvania State University and at Juniata College, as well as presentations on general principles of weathering, acid generation, and methods of prevention and treatment. Results of USGS studies on mineralogical controls on acid-rock drainage at Skytop were summarized at the conference and are presented in this report, along with other data for rock and water samples collected during site visits between May and September of 2004. This research was conducted as part of ongoing USGS studies of the geoenvironmental behavior of mineral deposits, the characterization of mine drainage, and modeling of near-surface processes.

Cover photo

Aerial view of the Skytop cut on January 6, 2005 looking north. Existing Route 322 in foreground. Future I99 roadbed runs along the base of the cut. Black plastic covers one of several areas of pyritic fill as a stopgap measure to minimize water infiltration. Photograph by Keith Brady.

Acid-rock drainage at Skytop, Centre County, Pennsylvania, 2004

By Jane M. Hammarstrom, Keith Brady, and Charles A. Cravotta III

Abstract

Recent construction for Interstate Highway 99 (I-99) exposed pyrite and associated Zn-Pb sulfide minerals beneath a >10-m thick gossan to oxidative weathering along a 40-60-m deep roadcut through a 270-m long section of the Ordovician Bald Eagle Formation at Skytop, near State College, Centre County, Pennsylvania. Nearby Zn-Pb deposits hosted in associated sandstone and limestone in Blair and Centre Counties were prospected in the past; however, these deposits generally were not viable as commercial mines. The pyritic sandstone from the roadcut was crushed and used locally as road base and fill for adjoining segments of I-99. Within months, acidic (pH<3), metal-laden seeps and runoff from the exposed cut and crushed sandstone raised concerns about surface- and ground-water contamination and prompted a halt in road construction and the beginning of costly remediation. Mineralized sandstones from the cut contain as much as 34 wt. % Fe, 28 wt. % S, 3.5 wt. % Zn, 1% wt. Pb, 88 ppm As, and 32 ppm Cd. A composite of <2 mm material sampled from the cut face contains 8.1 wt. % total sulfide S, 0.6 wt. % sulfate S, and is net acidic by acid-base accounting (net neutralization potential –234 kg $CaCO_3$/t). Primary sulfide minerals include pyrite, marcasite, sphalerite (2 to 12 wt. % Fe) and traces of chalcopyrite and galena. Pyrite occurs in mm- to cm-scale veinlets and disseminated grains in sandstone, as needles, and in a locally massive pyrite-cemented breccia along a fault. Inclusions (<10 μm) of CdS and Ni-Co-As minerals in pyrite and minor amounts of Cd in sphalerite (0.1 wt. % or less) explain the primary source of trace metals in the rock and in associated secondary minerals and seepage. Wet/dry cycles associated with intermittent rainfall promoted oxidative weathering and dissolution of primary sulfides and their oxidation products. Resulting sulfate solutions evaporated during dry periods to form intermittent "blooms" of soluble, yellow and white efflorescent sulfate salts (copiapite, melanterite, and halotrichite) on exposed rock and other surfaces. Salts coating the cut face incorporated Fe, Al, S, and minor Zn. They readily dissolved in deionized water in the laboratory to form solutions with pH <2.5, consistent with field observations. In addition to elevated dissolved Fe and sulfate concentrations (>1,000 mg/L), seep waters at the base of the cut contain >100 mg/L dissolved Zn and >1 mg/L As, Co, Cu, and Ni. Lead is relatively immobile (<10 μg/L in seep waters). The salts sequester metals and acidity between rainfall events. Episodic salt dissolution then contributes pulses of contamination including acid to surface runoff and ground water. The Skytop experience highlights the need to understand dynamic interactions of mineralogy and hydrology in order to avoid potentially negative environmental impacts associated with excavation in sulfidic rocks.

Contents

LIST OF FIGURES

TABLES

Introduction

Acid-rock drainage is the water-quality hazard resulting from the oxidation of iron sulfide minerals (Nordstrom and Alpers, 1999). The pH of acid-rock drainage typically ranges from 2 to 4, but can range to values as high as 8 and as low as -5 (Plumlee and others, 1999; Nordstrom and Alpers, 1999). Many metals are more mobile under acidic conditions when compared to neutral or alkaline conditions. Consequently, acid-rock drainage can contribute metals as well as acidity to water supplies and aquatic ecosystems. Acid-rock drainage that develops from ore, mine waste, or spoil piles associated with metal- or coal mines is called acid-mine drainage. Acid-mine drainage is a worldwide environmental problem (Nordstrom, 2000). The iron-sulfide minerals (pyrite, marcasite, pyrrhotite) that cause acid-mine drainage occur in many types of mineral deposits, coal-bearing rocks, rocks unrelated to mineral or coal deposits, and in acid sulfate soils. When these iron-sulfide minerals are exposed to oxidative weathering processes by natural or human-induced conditions, such as landslides or construction projects, acid-rock drainage may develop.

An acid-rock drainage problem developed at Skytop along Bald Eagle Mountain in central Pennsylvania, where construction of a new section of Interstate Highway 99 (I-99) between Port Matilda and State College exposed pyrite-rich rocks associated with a zinc-lead deposit within a sandstone ridge. A small gossan was exposed at the surface at Skytop and, although zinc and lead occurrences had been reported nearby, the extent of the pyrite veining and other sulfide mineralization encountered during excavation was unanticipated. More than a million cubic yards of material was excavated at the site starting in 2002. Approximately 70 meters (250 ft) of material was removed vertically along a 270-meter (900 ft) long section of rock. Some of the sandstone was crushed and used as roadway sub-base material. Most of the material was placed in designated fill areas adjacent to the new road. By September of 2003, acid seeps and surface runoff were emanating from the cut as well as from the fill and other areas where the pyritic rock had been distributed. Recognition of the severity of the problem prompted concerns about surface- and ground-water contamination because streams originate in the area and local residents depend on well water. Buffalo Run, the stream most directly affected by the acid-drainage problem, is a Class A trout stream in the Spring Creek watershed (Commonwealth of Pennsylvania, 2002). The Pennsylvania Department of Transportation (PennDOT) and the Pennsylvania Department of Environmental Protection initiated several activities to contain the problem until a long-term solution is implemented starting in 2005. Recent (2004) and ongoing site activities include detailed mapping and characterization of acid-generating materials, installation of monitoring wells and ground-water sampling, surface-water collection and active treatment, stream diversion, addition of lime kiln dust, and installation of a PVC cover over fill piles to divert surface runoff. Detailed maps of the site and information about road construction and the acid-drainage problem are available from the Pennsylvania Department of Transportation (2005) at: www.dot.state.pa.us. The history of site activities and community concerns are documented in a series of newspaper articles by Mike Joseph in the Centre Daily Times (Joseph, 2004a-e; 2005)

This report includes mineralogical and geochemical data for samples of pyritic rock and secondary minerals collected from the Skytop roadcut and water chemistry of acidic seeps sampled in May 2004 (prior to cut amendments and cover emplacement on fill). These data allow us to address questions, such as:

- What are the sources of acid and metals at Skytop?
- What processes caused the acid drainage to develop at Skytop?
- What is the water quality of the acid drainage at Skytop?

Geologic setting and site descriptions

The Skytop site is located on Bald Eagle Mountain along State Route 322 west of State College in Centre County, Pennsylvania (Fig. 1). Bald Eagle Mountain is a northeast- trending ridge that extends for over 100 kilometers along the Allegheny Front at the northwestern edge of the Valley and Ridge physiographic province. Near State College, the sedimentary rocks that constitute the ridges (Bald Eagle Mountain, Nittany Mountain) include the Ordovician Reedsville Shale, sandstones of the Ordovician Bald Eagle Formation, sandstone of the Ordovician Juniata Formation, and quartzite of the Silurian Tuscarora Formation. Bald Eagle Mountain forms the northwestern flank of the Nittany Anticlinoriom, a 10-km wide belt of complexly folded and eroded Paleozoic carbonate and silicate rocks (Nickelsen and others, 1989). Carbonate rocks are exposed in the Nittany Valley east of Bald Eagle Mountain (Fig. 1).

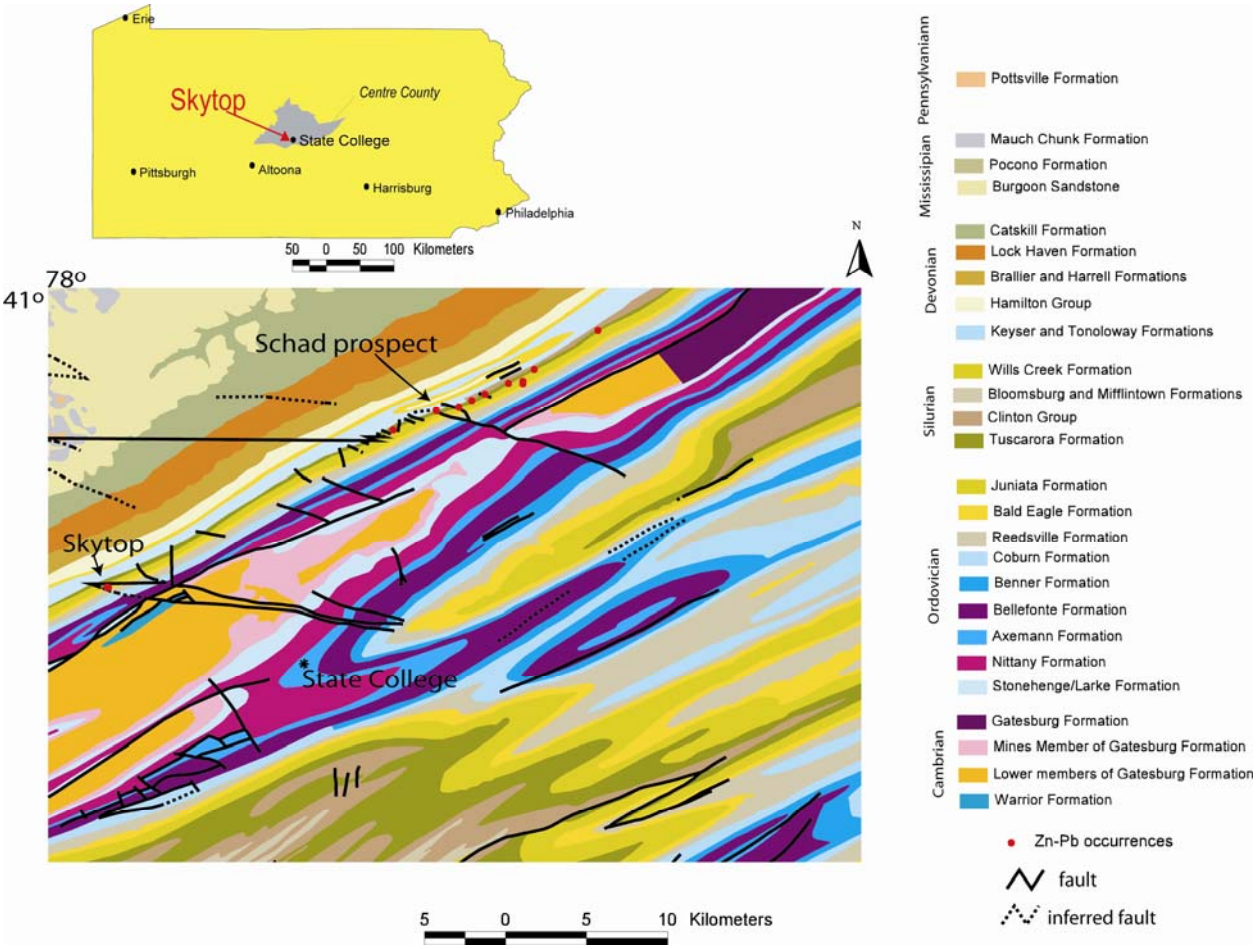

Figure 1. Geology of the northwestern corner of the State College 1: 250,000-scale quadrangle showing the distribution of Zn-Pb occurrences. Carbonate rocks are shown in blues (limestone) and purples (dolomite). Other rock types include sandstone, siltstone, mudstone, quartzite, and shale. The Zn-Pb occurrences shown are all associated with the silicic rocks (Bald Eagle, Juniata, and Tuscarora Formations). Simplified from the digital data set "Bedrock geology of Pennsylvania" (Miles and others, 2001), based on Berg and others (1980) and references therein. Preliminary 1:24,000-scale geologic maps for the Julian (Skytop) and Bellefonte (Schad prospect) quadrangles were used for the bedrock geology map (Berg and Dodge, 1981).

Smith (1977) described a number of zinc-lead prospects in quartzite of the Tuscarora Formation along Bald Eagle Mountain in the Milesburg Gap area of Centre County, about 24 km north of Skytop (Fig. 1) in the Mingoville and Bellefonte 7.5' quadrangles. In his description of the Milesburg Gap area, Smith (1977) also noted occurrences of galena, barite, and pyrite veins in the Bald Eagle Formation and in the Tuscarora Formation at Skytop in the Julian 7.5' quadrangle. However, it was not until the I-99 highway excavation at Skytop exposed extensive pyrite veins underlying the oxidized gossan zone along Route 322 that the extent of the Skytop occurrence was known.

Lead and zinc were mined in Pennsylvania from Revolutionary War times until the 1980s. Significant deposits are replacement- and breccia deposits hosted by carbonate rocks in the Valley and Ridge province and in the Piedmont of southeastern Pennsylvania. Rose (1999) presented an overview of metallic minerals deposits of zinc-lead-and silver in Pennsylvania. Smith (1977) provided a comprehensive description of zinc and lead occurrences throughout the state, updating an earlier report by Miller (1924). Additional studies of lead and zinc in central Pennsylvania by Smith (2003) address the nature and origin of lead and zinc in the Sinking Valley deposits in Blair County, which borders Centre County to the south. The Skytop and Milesburg occurrences of zinc and lead minerals are hosted by sandstones and quartzite rather than by carbonate rocks that host the Sinking Valley deposits. Pyrite veins are not associated with the Sinking Valley deposits. The structural geology, age, and

conditions of formation of the mineralization at Skytop and genetic links to other zinc-lead occurrences in the state are the focus of ongoing studies (Gold and others, 2005; Detrie and others, 2005; Sicree, 2005).

The Skytop site is along sections A12 and C12 of the Interstate 99 highway construction project between Port Matilda and State College, which will reroute the existing Route 322 corridor and improve access to State College (Fig. 2). Bald Eagle Creek lies north of sections A12 and C12. Buffalo Run and its tributaries flow through section A12 (Fig. 2). Parts of Buffalo Run have been diverted to protect the watershed from acid drainage from the construction site. Buffalo Run flows into Spring Creek, which flows into Bald Eagle Creek and eventually discharges into the Susquehanna River.

The Skytop cut in section A12 (Fig. 3A) exposes three Upper Ordovician rock units. From west to east, the cut exposes Juniata Formation, Bald Eagle Formation, and Reedsville Shale. The Bald Eagle Formation typically is a gray to olive-gray crossbedded sandstone, siltstone, and shale. In the Skytop cut, the sandstone is bleached an atypical white color (Dr. David Gold, Pennsylvania State University, oral commun., 2004). Quartzite of the Silurian Tuscarora Formation crops out in section C12, west of the cut area. Pyrite veins are most extensive in the Bald Eagle Formation near the center of the cut (Fig. 3B). Pyrite veinlets, white barite, and pink ankerite veins are present in bedrock exposed along section A12. The upper part of the cut is oxidized to a depth of >10 meters. Boulders of oxidized pyritic rock (gossan) are piled along Route 322 at the new overpass (Fig. 3C). Gold and others (2005) describe the stratigraphy and structure of the cut area; the pyrite veins generally trend north-northwest, have cut across bedding, and are displaced by a late fault.

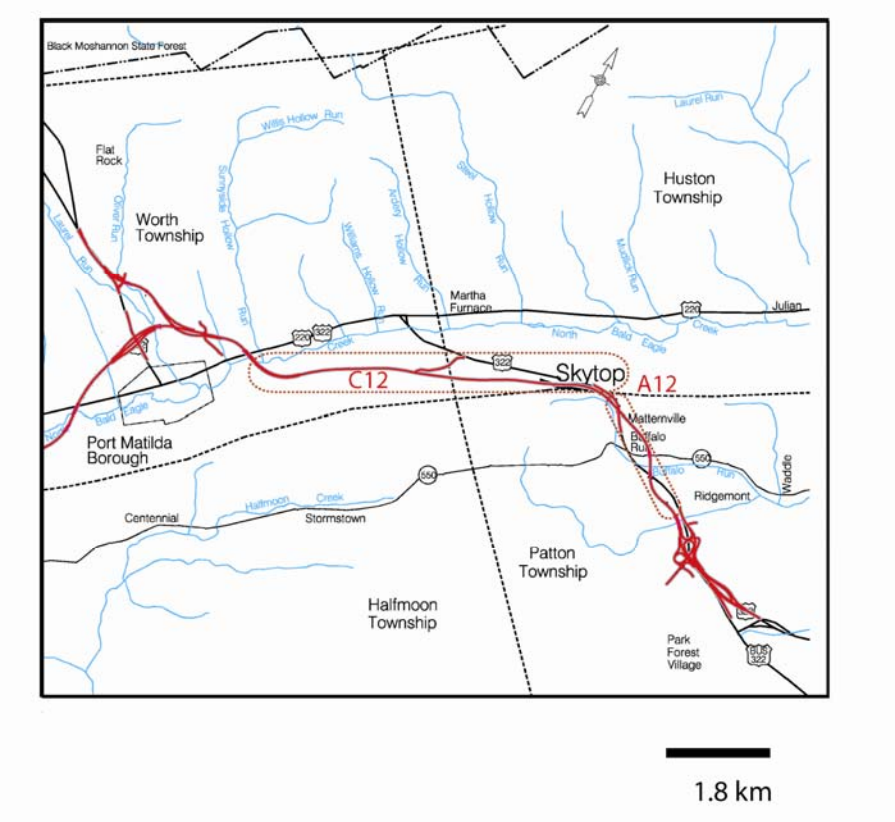

Figure 2. Map of the Skytop site. Red lines indicate new highway construction. Area A12 includes the Skytop cut area. Material excavated from section A12 was used as road base and slope fill along parts of section C12. Simplified from a map compiled for the Pennsylvania Department of Transportation (Skelly and Loy, Inc., 2004).

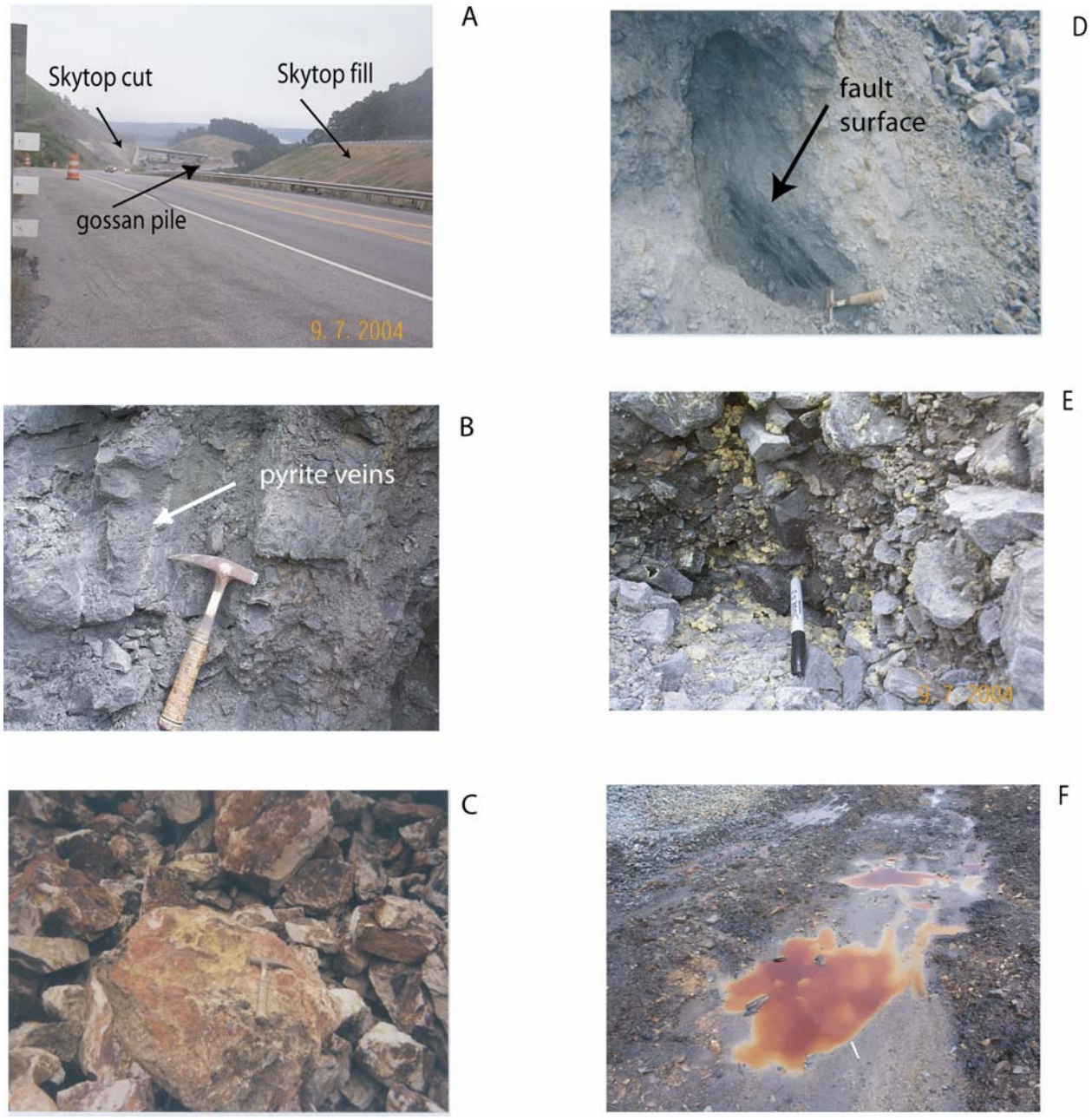

Figure 3. Field photographs. A, View of the Skytop cut and fill areas looking east from Skytop summit along Rt. 322. The bridge will carry rerouted Rt. 322 over new I-99. The gossan is in large boulders on the north side of Rt. 322 at the bridge. B, Pyrite veins in the Skytop cut. C, Gossan. D, Fault surface showing slickenliines. Note the polished (black) face developed on massive pyrite along the fault zone. E. Yellow (copiapite) and white (rozenite) efflorescent sulfate salts at the Skytop cut. F, Acid puddle at the base of the Arbogast pile of material excavated from the Skytop cut.

Several forms of pyrite have been identified at the site. Sicree (2005) described "bright" pyrite veins, "dull" pyrite, and clusters of "whisker" pyrite that grew on terminated quartz crystals. The terms "bright" and "dull" refer to the luster of the pyrite. Coarse crystals of dark colored sphalerite and more rarely galena can be found, especially in piles of excavated material. A zone of massive sulfide occurs locally along a fault that has cut through the section, where the fault created a natural polish and slickenlines on pyrite (Fig. 3D). The Skytop site was visited three times for this study between May and September of 2004, before the Skytop fill area was covered with PVC sheeting. A variety of rock samples were collected along the base of the cut and from excavated piles in section A12. Outcrop samples were collected from the north side of the cut in section A12 between marker posts 154 (40° 49.986" N, 77° 58.033" W) and 162 and at the fault zone near marker post 370 (40° 49.973" N, 77° 57.986" W). At the level of the road base, whisker pyrites were best exposed near marker post 162, and veins were best developed near marker post 370. A composite sample of soil (<2 mm material) was collected from the lower part of the cut, about a meter above the surveying flags between marker posts 154 and 370 for chemistry and acid-base accounting. The cut face consists of bedrock, soil, and fist-size pieces of rock. Where the rock is pyritic, exposed bedrock is rapidly deteriorating to a crumbly mass. In June, yellow and white efflorescent salts were locally developed in the damp, partly sheltered soil at the fault zone. In September however, salts were ubiquitous on rocks and soil along the entire west end of the cut (Fig. 3E). Salts were sampled in June and September for mineralogy. According to regular visitors to the site, the salts can be even more abundant than we observed depending on the weather. PennDOT workers also report variations in pH of surface runoff into treatment ponds following rain events, which are consistent with periodic flushing and regrowth of the highly soluble salts from the cut face and fill piles. Seep waters emanating from the Skytop fill and the Arbogast stockpile were sampled in May of 2004. In June, a number of red, acidic puddles were observed on the site (Fig. 3F).

The Milesburg Gap occurrences consist of varying amounts of sphalerite, galena, and chalcopyrite in a gangue of quartz, barite, and limonite (Smith, 1977). Butts and Moore (1936) noted that lead, zinc, silver, and barite occur in the Bellefonte quadrangle in amounts too small to be of commercial interest. Site workings consisted of pits and trenches at most of the occurrences. The most developed property was the Schad prospect where a horizontal adit was driven in 1915. Additional site development was done 1938-1941, and again in 1954. Butts and Moore (1936) described the Schad prospect as a "ganister" (local term for industrial-grade silica rock) quarry in Tuscarora quartzite, where a 15-m drift explored a 15-cm vein of galena, pyromorphite, red sphalerite, barite, and minor silver in a clay and barite gangue. Assays of ore from 1941 reported as much as 13% zinc, 24 % lead, and minor silver; geochemical data for composites of limonite-quartzite sampled in 1976 contained as much as 5,000 ppm arsenic (Smith, 1977). The Schad adit was bulldozed closed and only a small dump (<10 m in diameter) remained when the site was visited in June 2004. No seeps were noted. Representative ore samples were collected for comparison with Skytop samples.

A number of other studies mention zinc-lead mineralization near Skytop. Krohn (1979) examined the field relations of lineaments to gossans and geochemical anomalies along Bald Eagle Mountain. He suggested that the deposits of Bald Eagle Mountain may be analogous to the Wurtsboro-type of lead-zinc deposits in New York, which are in quartzite and conglomerate of the Silurian Shawangunk Formation (partly equivalent to the Tuscarora Formation). Hsu (1973) detected anomalous concentrations of zinc in stream sediments in the Mingoville quadrangle. Illsley (1955) reported anomalous zinc and other heavy metals in a tributary to Buffalo Run that decreased in concentration after rain. All of these indications of mineralization led Smith (1977) to conclude that the area warranted further exploration for zinc and lead. Subsequently, Howe and others (1979) and Howe (1981, 1988) studied the mineralogy, fluid inclusions and sulfur isotopes of lead-zinc occurrences in central Pennsylvania. Howe (1988) noted that epigenetic lead-zinc deposits occur over a 5,000 km^2 area and that the Skytop and Milesburg Gap areas were among the most strongly mineralized areas that might warrant further exploration.

Methods

Rock geochemistry

Samples of pyritic sandstone from the Skytop cut and ore from the mine dump at the Schad prospect were submitted to USGS Analytical Laboratories for sample preparation. Major elements were analyzed by wavelength-dispersive X-ray fluorescence spectroscopy (WD-XRF) in USGS Laboratories in Denver, CO. Sample preparation, analytical methods, and detection limits are reported in Taggart (2002). All other analyses were done at XRAL Laboratories under contract to the USGS. Forty-two major-, minor-, and trace elements were determined by inductively coupled plasma-atomic emission spectrometry (ICP-AES) and inductively coupled plasma-mass

spectrometry (ICP-MS). Other analyses included gold determined by fire assay, total sulfur by LECO furnace, and total and carbonate carbon using an automated carbon analyzer. Details of the XRAL analytical methods are given in the Appendix. The composite (>1 kg) soil sample from the Skytop cut was analyzed for acid-base accounting by Vizon SciTec, Inc. of Vancouver, British Columbia using the standard Sobek method (Sobek and others, 1978). Multi-element ICP-AES and ICP-MS and gold analyses were obtained for the soil composite using the same methods as described above.

Leach test

A leach test (Hageman and Briggs, 2000) was done on a 50-gram split of the composite soil sample from the Skytop cut. The leach test was developed as a field test to indicate the potential chemical composition of surface run-off from the weathered surfaces of mine waste piles. The test has been adapted for lab use as a screening tool for qualitative assessment of mine wastes at several mine sites in the eastern United States (Hammarstrom and others, 2003a,b; Piatak and others, 2004). The Skytop soil (<2 mm particle size) was combined with a solution that approximates precipitation in the eastern United States. The solution was prepared with sulfuric and nitric acids to a pH of 4.2 ± 0.1, and then added to the soil in a 20:1 ratio of solution to soil. The mixture was shaken for five minutes; after 24 hours, the pH and specific conductance were measured on unfiltered splits. The leachate was then filtered (0.45 μm pore-size nitrocellulose filter) and analyzed for cations by inductively coupled plasma-mass spectrometry (ICP-MS) and inductively coupled plasma-atomic emission spectrometry (ICP-AES), and for anions by ion chromatography in USGS laboratories in Denver, Colorado. Dissolved total iron and ferrous iron were determined using colorimetric kits on a Hach DR/2000 spectrophotometer.

Mineralogy

Rocks were cut and prepared as polished thin sections for optical microscopy, scanning electron microscopy (SEM), and electron probe microanalysis (EPMA). Hand-picked mineral concentrates were analyzed by powder X-ray diffraction (XRD) as smear mounts on quartz plates. Powder patterns were collected on a Scintag X1 automated diffractometer equipped with a Peltier detector using CuKα radiation. Patterns were interpreted with the aid of Scintag and MDI Applications JADE search/match software and compared with reference patterns in the Powder Diffraction File (ICDD, 2002).

Efflorescent sulfate salts were hand-picked under a binocular microscope and affixed to glass slides with epoxy. Salts and thin sections were carbon-coated and examined with a JEOL JSM-840 scanning electron microscope (SEM) equipped with a back-scattered electron (BSE) detector, a secondary electron (SE) detector, and a PGT X-ray energy-dispersive system (EDS). EDS spectra were collected to obtain a qualitative analysis of mineral compositions to refine XRD identifications. The SEM typically was operated at an accelerating voltage of 15 kV and a specimen current of 1 to 2 nA. Sulfide minerals were analyzed for 16 elements by EPMA using a JEOL electron microprobe optimized for determining trace-element concentrations in sulfide minerals by operating at 20 kV, 50 nA, and using long (60 second) peak count times. Detection limits based on counting statistics are on the order of 200 ppm or less. Standards included a variety of natural and synthetic sulfide minerals. The SEM and EPMA instruments are in USGS laboratories in Reston, VA.

Seep waters

Four seep-water samples were collected in May of 2004 after several days of dry weather. Data for flow rate, temperature, specific conductance (SC), pH, and redox potential (Eh) were measured at each site using standard methods (U.S. Geological Survey, 1997 to present). Flow rate was measured volumetrically with a stopwatch and calibrated vessel. All meters were calibrated in the field using electrodes and standards that had been thermally equilibrated to sample temperatures. The SC was measured with a Wheatstone bridge calibrated in 5,000 μS/cm potassium chloride solution. The pH was measured with a liquid junction Ag/AgCl electrode calibrated in pH 2.0, 4.0, and 7.0 buffers. Eh was determined using a combination Pt and Ag/AgCl electrode calibrated in Zobell's solution and corrected to 25 °C according to methods of Nordstrom (1977). Water samples were collected as 1-liter grab samples and split into subsamples for filtration and preservation. Filtered (0.45- μm pore-size filter) samples for anion analysis were stored in sample-rinsed polyethylene bottles; filtered samples for dissolved metal analysis

were acidified with nitric acid and stored in sample-rinsed polyethylene bottles. Water samples were submitted to Activation Laboratories Ltd. for analysis of major elements by inductively coupled plasma optical emission spectrometry (ICP-OES), trace elements by inductively coupled plasma-mass spectrometry (ICP-MS), and anions by ion chromatography (IC).

Results

Geochemical and mineralogical data are summarized in a series of tables (Table 1-6). Results are presented by sample media.

Rock samples

Whole-rock geochemical data were acquired for three samples of pyritic rock from the Skytop cut and one sample of coarse-grained ore from the mine dump at the Schad prospect. The Skytop samples include massive pyrite (sample Skytop-1), competent sandstone cut by mm-scale pyrite veinlets (Skytop-6), and friable black rock from the fault zone (Skytop-10). These samples are not representative of the entire cut face, but were selected to document the geochemical signature of the most pyritic rocks exposed near the base of the cut. The Schad sample contains visible sphalerite and galena and lacks pyrite veins. Iron, sulfur, and silica were the major constituents of all samples (Table 1). Concentrations of aluminum are <2 wt. % and concentrations of calcium, sodium, potassium, and magnesium are all extremely low (<1 wt. %). The low silica content (18 wt. % SiO_2) of sample Skytop-1 relative to the other Skytop rocks (> 45 wt. % SiO_2) reflects the pyrite-rich character of the massive sulfide sample. Zinc (0.1 to 4 wt. % Zn) exceeded lead (0.02 to 1.5 wt. % Pb) in all samples; copper was present in concentrations of 157 ppm Cu or less. In addition to zinc and lead, some trace elements were present in the Skytop samples well in excess of crustal abundances (Table 1b). Table 1b includes an analysis of ore from the Valzinco lead-zinc mine in Virginia for comparison; the Skytop samples contain comparable or higher concentrations of lead. In addition to lead and zinc, trace elements of potential environmental concern (that is, if mobilized from rock to water) in the Skytop samples are as follows: arsenic (61 to 88 ppm), cadmium (1.5 to 32 ppm), and thallium (2.9 to 4.5 ppm). The pyrite-veined sandstone sample (Skytop-6) contains higher concentrations of zinc and lead than the massive pyrite (Skytop-1) and fault gouge (Skytop-10) samples.

Table 1. Geochemical data for mineralized rocks.

A. Major elements

[Oxides determined by WD-XRF; total iron reported as Fe_2O_3; LOI, loss on ignition; I; interference with high Zn; see text for other methods]

Sample	Skytop 1	Skytop 6	Skytop 10	Schad 1
	Weight percent			
SiO_2	18.01	46.03	55.84	67.89
Al_2O_3	1.66	1.73	2.75	0.62
Fe_2O_3	52.66	23.07	20.06	0.69
MgO	0.19	0.15	0.2	0.1
TiO_2	0.13	0.14	0.15	0.2
MnO	<0.01	0.02	0.01	0.03
Cr_2O_3	<0.01	<0.01	<0.01	<0.01
CaO	<0.01	<0.01	<0.01	<0.01
K_2O	0.33	0.46	0.75	0.23
Na_2O	<0.01	I	I	I
P_2O_5	0.06	0.08	0.04	0.02
LOI	27.45	14.7	12.05	2.55
S	42.5	22.8	19.1	5.1
Total CO_2	0.01	0.02	0.01	0.02
Carbonate C	<0.003	0.01	<0.003	0.01

B. Major-, minor- and trace elements determined by ICP-MS and ICP-AES

[Valzinco ore sample from the Valzinco Zn-Pb mine, VA (Hammarstrom and others, in prep.); Clarke values represent the average abundance of an element in the lithosphere (Fortescue, 1992)]

Sample	Skytop-1	Skytop-6	Skytop-10	Schad-1	Valzinco ore	Clarke values
Element concentrations in weight percent						
Al	0.86	0.97	1.55	0.35	0.13	8.4
Ca	<0.01	<0.01	<0.01	0.01	0.1	4.7
Fe	33.81	16.67	13.85	0.5	54	6.2
K	0.22	0.34	0.61	0.16	<0.05	1.8
Mg	0.03	0.04	0.08	0.04	0.62	2.8
Na	<0.01	0.01	0.01	<0.01	2.23	2.3
S	28.13	18.13	15.37	3.69	38.1	0.03
Ti	0.03	0.02	0.03	0.02	<0.01	0.6
Element concentrations in parts per million						
Au	0.009	<0.005	<0.005	<0.005	n.d.	0.004
Ag	2	3	1	7	4.4	0.08
As	88	85	61	76	62	1.8
Ba	77	92	59	221	8.3	390
Be	0.2	0.2	0.2	<0.1	n.d.	2
Bi	<0.04	<0.04	<0.04	0.07	0.26	0.0082
Cd	1.5	32	16.7	36.9	160	0.16
Ce	7.05	4.4	4.79	3.84	2	66.4
Co	16.5	7.8	11.7	1.8	450	29
Cr	9	7	10	4	n.d.	122
Cs	0.54	0.49	0.89	0.31	0.1	2.6
Cu	104.6	141.3	90	157.2	15,000	68
Ga	14.8	20.5	19.2	21	3.2	19
In	0.02	0.05	0.27	0.24	67	0.24
La	3	1.8	3.1	1.4	1.2	34.6
Li	13	22	30	31	n.d.	18
Mn	32	40	50	11	4,800	1,060
Mo	0.36	0.4	0.7	0.29	28	1.2
Nb	0.7	0.5	0.6	0.7	<1	20
Ni	15.2	13.5	22.1	4.1	100	99
P	91	170	<50	<50	<900	1,120
Pb	775.5	10,425	245.5	15,496	260	13
Rb	7.9	10.1	18.2	5.5	3.6	78
Sb	10.3	6.78	4.88	11	4.2	0.2
Sc	0.9	1.4	2.5	0.6	<0.5	25
Sn	0.4	0.4	0.6	1.9	33	2.1
Sr	11.6	9.5	9.3	174.9	<5	384
Te	<0.1	<0.1	<0.1	<0.1	n.d.	0.004
Th	2.6	1.3	1.7	1	<0.5	8.1
Tl	4.5	3.9	2.9	0.3	<2	0.72
U	1.3	1	0.7	0.3	0.32	2.3
V	10	13	21	5	7.2	136
W	1	1	1.1	0.2	0.61	1.2
Y	3.9	5.9	3.8	1.9	2.9	31
Zn	1,100	35,060	24,590	41,920	69,000	76

Soil composite

Soil-size (<2 mm) material was sampled near the base of the cut face approximately one meter above the roadbed. This material is not a typical soil formed by long-term surface weathering of bedrock. It is the material that is forming as the exposed bedrock weathers and may include material eroded from the upper part of the cut that has washed down slope as well as material redistributed by construction activities. The soil sample contains 8.4 wt. % S, 8.1 wt. % Fe, 4.6 wt. % Al, and 1.6 wt. % Ca (Table 2a). Silicon, the major constituent of the sandstone, was not determined. The amount of total sulfur determined in the acid-base accounting sample split (8.6 wt. %) is in excellent agreement with the total sulfur reported for the geochemistry sample split. Relative to the rock samples (Table 1), the soil has higher concentrations of Al, K, Ca, P, and Sr and lower concentrations of Fe and S. These differences reflect the heterogeneity of the outcrop, the weathering process, and the incorporation of limestone used for treatment. Shale inclusions are the likely source of the Al and K; limestone is the likely source of the Ca and Sr. Although total concentrations of metals are lower in soil than in individual rock samples, the soil contains somewhat anomalous concentrations of some metals: 788 ppm Zn, 229 ppm Pb, and 62 ppm Cu, as well as 36 ppm As. These concentrations exceed mean element concentrations for eastern U.S. soils. However, the element concentrations lie within observed concentration ranges. Arsenic exceeds the U.S. EPA (2004) preliminary remediation goal for residential (0.39 ppm) and industrial (1.6 ppm) soils, and also exceeds the soil screening level for migration to groundwater (29 ppm for a dilution attenuation factor of 20). Concentrations in excess of these soil screening guidelines suggest that further evaluation of a potential risk is warranted.

Acid-base accounting for the composite soil sample shows that the material is net acid-generating (Table 2b). Quartz (~62 %), pyrite (16%), marcasite (11%), with minor amounts of mica and sphalerite and traces of gypsum and calcite are detected by XRD. Mineral percentages are rough estimates based on XRD pattern analysis. The calcite explains the slight fizz and high paste pH value. The calcite is a contaminant from neutralizing materials applied nearby; no calcite is observed in any of the rock samples collected from the Skytop cut. Gypsum probably formed from reaction of calcite with sulfate in soil pore waters. Despite the presence of the calcite, the soil material developing near the base of the cut is classified as strongly acid-generating by criteria used for interpreting acid-base accounting results because the net neutralization potential is negative and the ratio of neutralization potential (NP) to potential acidity (AP) is <1 (Sobek and others, 1978; U.S. EPA, 1994).

The leach test shows that Fe, Al, Zn, Cd, Ni, and sulfate are readily released from the soil (Table 2c). Complete leachate data are listed in Appendix B. Some soil leachate metal concentrations exceed U.S. EPA (2004) national recommended water quality criteria for priority toxic pollutants for freshwater aquatic life. The leachate sulfate concentration (1,657mg/L) is well in excess of the U.S. EPA secondary drinking water standard for sulfate (250 mg/L); the Al concentration (22.9 mg/L) exceeds the Commonwealth of Pennsylvania (1998) maximum concentration of aluminum in effluent from an active mine (0.75 mg/L). During the leach test, the solution pH decreased from 4.2 to about 4.1. Paste pH measured 3.9 on the leachate sample split. The relatively high paste pH (7.2) and calcite detected in the acid-base accounting subsample most likely reflects sample heterogeneity. Water quality standards for Pennsylvania require pH in the range 6.0 to 9.0 and maximum sulfate concentrations of 250 mg/L (Commonwealth of Pennsylvania, 2005).

Table 2. Skytop soil composite.

A. Soil chemistry.

[Eastern U.S. soils data from Shacklette and Boerngen, 1984; -, not reported]

Sample	Skytop-19	Eastern U.S. soils	
		Mean	Range
Element concentrations in weight percent			
Al	4.61	3.3	0.7 - >10
Ca	1.63	0.34	0.01 - 28
Fe	8.13	1.4	0.01 - >10
K	1.73	1.2	0.005 - 3.7
Mg	0.31	0.21	0.005 - 5
Na	0.02	0.25	<0.05 - 5
S	8.4	0.1	<0.08 – 0.31
Ti	0.19	0.28	0.007 – 1.5
Element concentrations in parts per million			
Au	<0.005	-	-
Ag	<1	-	-
As	36	4.8	<0.1 - 73
Ba	178	290	10 – 1,500
Be	0.9	0.55	<1 - 7
Bi	0.1	-	-
Cd	1.3	-	-
Ce	24.7	63	<150 - 300
Co	11.5	5.9	<0.3 - 70
Cr	29	33	1 – 1,000
Cs	2.79	-	-
Cu	61.7	13	<1 - 700
Ga	11.6	9.3	<5 - 70
In	0.06	-	-
La	10.3	29	<30 - 200
Li	21	17	<5 - 140
Mn	32	260	<2 – 7,000
Mo	0.5	0.32	<3 - 15
Nb	4.7	10	<10 - 50
Ni	41.8	11	<5 - 700
P	284	200	<20 – 6,800
Pb	228.6	14	<10 - 300
Rb	57.7	42	<20 - 160
Sb	3.24	0.52	<1 – 8.8
Sc	8.1	6.5	<5 - 30
Sn	1.1	0.86	<0.1 - 10
Sr	43.1	53	<5 - 700
Te	<0.1	-	-
Th	7	7.7	2.2 - 23
Tl	1.5	-	-
U	2.9	2.1	0.29 - 11
V	78	43	<7 - 300
W	0.6	-	-
Y	13.7	20	<10 - 200
Zn	788	40	<5 – 2,900

Table 2. Skytop soil composite.

B. Acid-base accounting.

Paste pH	7.2
Total sulfur (wt. %)	8.6
Sulfate sulfur (wt. %)	0.6
Sulfide sulfur (wt. %)	8.0
Maximum potential acidity (kg $CaCO_3$/t)	252
Neutralization potential (kg $CaCO_3$/t)	18
Net neutralization potential (kg $CaCO_3$/t)	-234
Fizz	slight

C. Soil leachate chemistry (selected elements).

[See Appendix B for complete leachate chemistry and analytical methods; U.S. EPA, National recommended water quality criteria for priority toxic pollutants for freshwater aquatic life (U.S. EPA, 2004). CMC, criteria maximum concentration; CCC, criterion continuous concentration for assumed hardness of 100 mg/L $CasCO_3$]

Element	Units	Concentration	EPA water quality criteria	
			CMC	CCC
SO_4	mg/L	1,657	-	-
Al	µg/L	22,900	-	-
As	µg/L	<1	340	150
Cd	µg/L	34.2	2	0.25
Co	µg/L	170	-	-
Cu	µg/L	397	13	9
Ni	µg/L	326	470	52
Pb	µg/L	0.2	65	2.5
Zn	µg/L	9,580	120	120

Mineralogy of the Skytop pyrite veins

Primary minerals include those that constitute the sandstone (mainly quartz) as well as those that were deposited from hydrothermal solutions that formed the mineral deposit (pyrite and other ore minerals). Secondary minerals were formed by the weathering of the primary minerals. Secondary minerals include the yellow and white sulfate salts that intermittently effloresce on rock and soil on the cut face and fill piles (Fig. 3E). Salts can be mistaken as organic material (lichen). The iron-sulfate salt minerals readily dissolve in water to produce an acidic solution. A simple field test can indicate the presence of these minerals: add a sample to a little water to see if it readily dissolves and check the solution pH with indicator paper or a meter. Other secondary minerals include iron oxide and iron oxyhydroxide minerals that form by weathering of pyrite; these minerals contribute the bright red, orange, and yellow colors to the gossan along Route 322 (Fig.3C). Minerals found at Skytop are listed in Table 3, along with their nominal chemical formulas.

Table 3. Skytop minerals

[Minerals are listed in alphabetical order]

Mineral	Chemical formula
Ankerite	$Ca(Fe,Mg,Mn)(CO_3)_2$
Alunogen	$Al_2(SO_4)_3 \bullet 17H_2O$
Barite	$BaSO_4$
chalcopyrite	$CuFeS_2$
Copiapite	$Fe^{2+}Fe^{3+}_4(SO_4)_6(OH)_2 \bullet 20H_2O$
Galena	PbS
Goethite	$Fe^{3+}O(OH)$
greenockite(?)	CdS
Gypsum	$CaSO_4 \bullet 2H_2O$
halotrichite	$FeAl_2(SO_4)_4 \bullet 22H_2O$
Hematite	Fe_2O_3
Jarosite	$K_2Fe^{3+}_6(SO_4)_4(OH)_{12}$
Marcasite	FeS_2
melanterite	$FeSO_4 \bullet 7H_2O$
Pyrite	FeS_2
Pyrrhotite	$Fe_{(1-x)}S$
Quartz	SiO_2
Rozenite	$FeSO_4 \bullet 4H_2O$
Rutile	TiO_2
Sphalerite	ZnS
Variscite	$AlPO_4 \bullet 2H_2O$
Wavellite	$Al_3(PO_4)_2(OH,F)_3 \bullet 5H_2O$
woodhouseite	$CaAl_3(PO_4)(SO_4)(OH)_6$
Xenotime	YPO_4
Zircon	$ZrSiO_4$

Primary minerals

Quartz is the most abundant mineral in all of the samples collected for this study. The Bald Eagle sandstone at Skytop is composed essentially of quartz. Minor amounts of mica were detected by XRD. Small (10 micrometer) crystals of zircon, xenotime, and monazite were identified by SEM (Fig. 4). EDS spectra and wavelength scans by EPMA show that xenotime has concentrated the heavy rare-earth elements (Dy, Gd, Er) whereas monazite has concentrated light rare-earth elements (Ce, Nd) as well as La and Th. Other phosphate minerals reported at Skytop include wavellite, variscite, and woodhouseite (Dr. Andrew A. Sicree, Pennsylvania State University , oral commun., 2004). Pyrite is ubiquitous in the rocks sampled from the Skytop cut for this study. The most common mode of occurrence of pyrite is in millimeter- to centimeter-wide veins that have cut sandstone. Pyrite has formed crosscutting and anastamosing veinlets throughout the sandstone, as well as euhedral veins of 1-millimeter-wide cubes of bright pyrite that clearly grew in open-space (Fig. 5A). Vein selvages and disseminated clots of pyrite in sandstone have a graphic texture, and some pyrite grew in an unusual, delicate needle or whisker form on terminated quartz crystals (Fig. 5B). The graphic texture probably reflects a variant of the needle pyrite habit. XRD analysis of massive sulfide sampled from the fault zone identified marcasite as well as pyrite. The pyrite:marcasite ratio in the massive sulfide is about 10:1, based on semiquantitative estimates of mineral

abundances using a Rietveld refinement on the full XRD profile. XRD patterns of bright and dull pyrite veins show that the bright veins are pure pyrite whereas the dull veins contain both pyrite and marcasite (Fig. 5C).

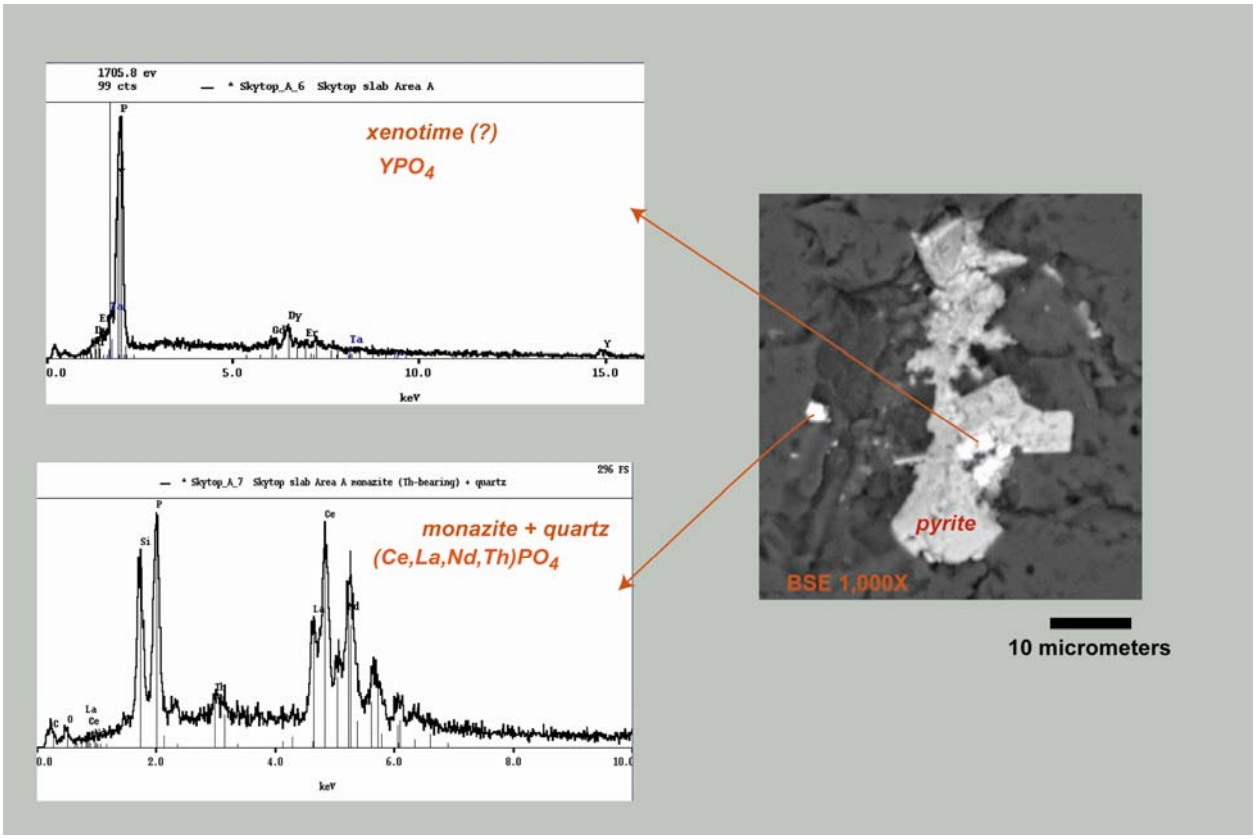

Figure 4. Phosphate minerals from pyritic Bald Eagle Formation. Identified by SEM. Backscattered-electron SEM image shows inclusions of xenotime in pyrite and monazite in quartz in Bald Eagle Formation. EDS spectra show that the ytrrium phosphate mineral xenotime (?) contains heavy rare-earth elements; monazite is enriched light rare-earth elements.

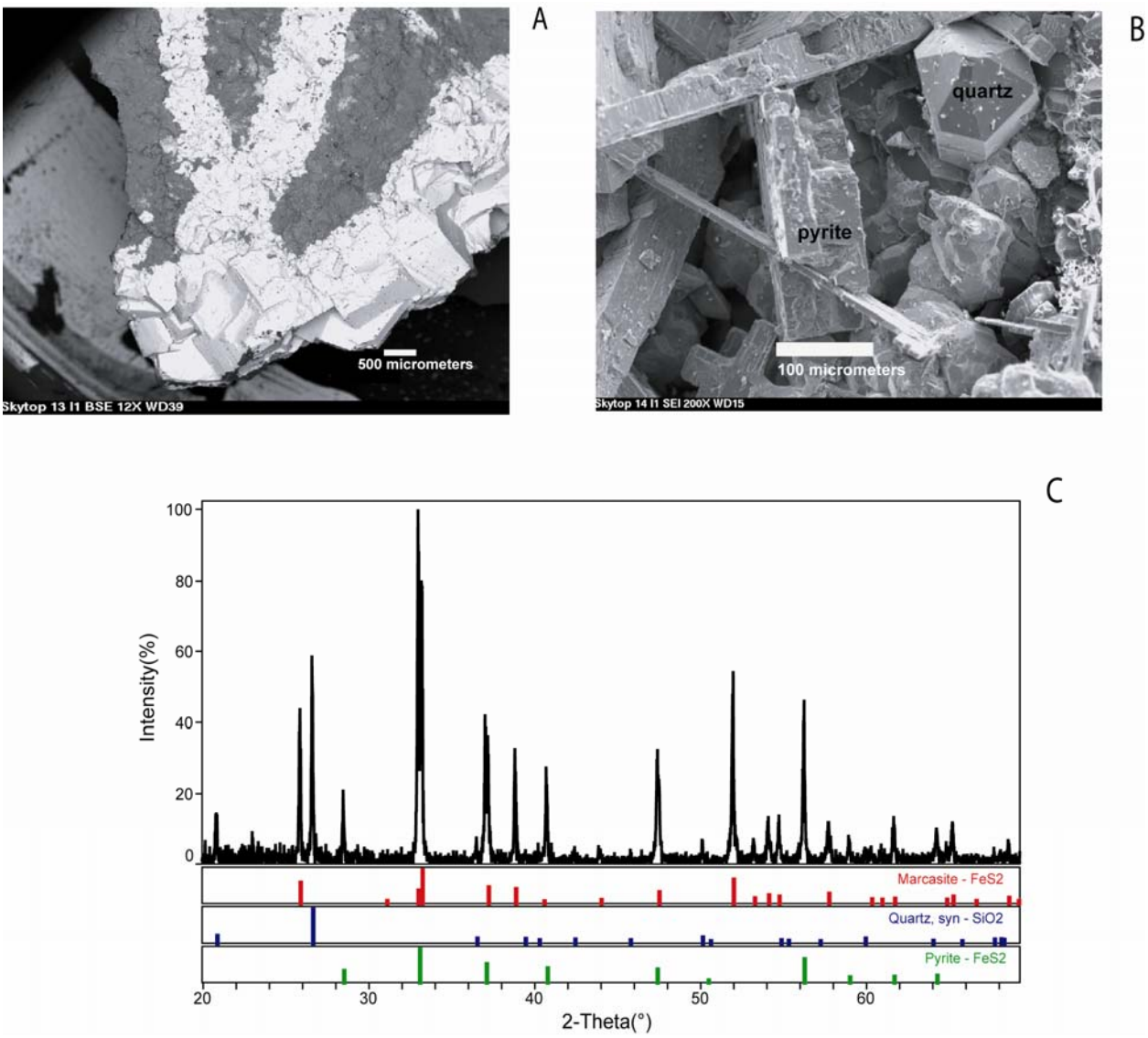

Figure 5. Pyrite. A, Intersecting veins of pyrite (white) cutting sandstone (gray). Euhedral pyrite cubes coarsen outward along the edge of the sample suggesting open-space growth. Backscattered-electron image at low magnification (12X). B, Whisker pyrite (confirmed by XRD) on terminated quartz crystals. Secondary-electron image at 200X. C, XRD pattern for massive sulfide from the fault zone shows that both pyrite and marcasite are present.

Massive, vein, and whisker pyrites were analyzed for a suite of 16 elements to search for compositional variations that might correlate with different types of pyrite (Table 4). At the detection limits of the EPMA method (0.01 to 0.03 wt. % for the operating conditions used), no trace-element enrichments were observed in any of the pyrites. In backscattered-electron mode, variations in brightness among pyrites suggest that there may be slight contrasts in average atomic number reflecting trace-element compositional variation within veins. Analytical methods such as laser ablation ICP-MS would be useful to investigate compositional variations among different types of pyrite at Skytop at lower detection limits. Bulk chemical analysis of pyrite separates may be a problem because tiny (<5 micrometer) inclusions of other minerals (mainly sphalerite) are present within many of the veins, especially in interior parts of the veins; thus, it would be difficult to get a pure pyrite sample for analysis. Bright pyrite, whisker pyrite, and graphic pyrite textures along vein selvages tend to contain fewer impurities than massive, brecciated, and vein pyrite associated with the fault zone. Figure 6 illustrates the variety of mineral inclusions tentatively identified in pyrite on the basis of their EDS spectra; inclusions are too small to extract for XRD analysis for confirmation of mineralogy. CdS can occur in two mineral forms, greenockite (hexagonal) and hawleyite (cubic). These minerals typically form as secondary coatings on sphalerite. At Skytop, CdS occurs as 10-micrometer blebs in chalcopyrite and in pyrite. Rare blebs of a Ni-skutterudite (?) are also observed; based on

Table 4. Pyrite compositions determined by electron probe microanalysis.

[N, number of analyses for each sample. Co concentrations are corrected for Fe interferences. Detection limits for all elements based on counting statistics range from < 0.01 to 0.03%]

Sample	Skytop 2 (mm-scale veins)		Skytop 3 (mm-scale veins)		Skytop 4 (vein, graphic)		Skytop 9 (dull vein)		Skytop slab (massive)		Skytop 14 (whisker)		Schad 1 (disseminated pyrite)		Schad 2 (1-cm clast)	
N	17		8		5		6		43		5		5		3	
	Avg	SD	Avg	SD	Avg	SD	Avg	SD	Avg	SD	Avg	SD	Avg	SD	Avg	SD
	Element (wt. %)															
Zn	0.00	0.01	0.01	0.02	0.01	0.01	0.01	0.01	0.00	0.00	0.00	0.01	0.00	0.01	0.00	0.01
Ni	0.01	0.01	0.00	0.00	0.00	0.00	0.01	0.01	0.00	0.01	0.00	0.00	0.05	0.07	0.03	0.05
Hg	0.00	0.00	0.00	0.00	0.00	0.00	0.00	0.00	0.00	0.00	0.00	0.00	0.00	0.00	0.00	0.00
S	53.0	0.2	52.5	0.2	52.9	0.1	52.9	0.2	53.4	1.2	52.2	0.2	53.0	0.1	52.4	0.6
Cu	0.04	0.03	0.02	0.02	0.01	0.01	0.05	0.02	0.01	0.02	0.01	0.01	0.01	0.02	0.01	0.02
Co	0.01	0.01	0.00	0.01	0.01	0.00	0.01	0.01	0.00	0.01	0.00	0.01	0.02	0.01	0.02	0.03
Ge	0.02	0.04	0.00	0.00	0.00	0.00	0.00	0.00	0.00	0.02	0.00	0.00	0.00	0.00	0.00	0.00
Pb	0.06	0.04	0.04	0.06	0.03	0.04	0.07	0.03	0.05	0.06	0.05	0.01	0.05	0.03	0.10	0.03
Fe	46.3	0.7	47.6	0.3	46.3	0.9	45.3	0.9	46.6	0.9	46.1	0.5	46.4	0.5	45.8	0.9
Te	0.00	0.00	0.01	0.01	0.00	0.01	0.00	0.01	0.00	0.00	0.01	0.01	0.00	0.01	0.00	0.01
As	0.00	0.00	0.02	0.01	0.00	0.00	0.00	0.00	0.01	0.01	0.00	0.00	0.01	0.02	0.12	0.21
Ag	0.00	0.00	0.00	0.00	0.00	0.00	0.00	0.00	0.00	0.00	0.00	0.01	0.00	0.01	0.01	0.01
Mn	0.00	0.01	0.03	0.01	0.00	0.00	0.00	0.01	0.06	0.07	0.00	0.00	0.00	0.00	0.00	0.00
Sb	0.00	0.00	0.00	0.00	0.00	0.00	0.01	0.01	0.00	0.00	0.01	0.00	0.00	0.00	0.01	0.01
Se	0.00	0.00	0.00	0.00	0.00	0.00	0.00	0.00	0.00	0.00	0.00	0.01	0.00	0.00	0.00	0.00
Cd	0.00	0.00	0.00	0.00	0.01	0.00	0.00	0.00	0.00	0.00	0.00	0.00	0.00	0.00	0.00	0.01
Total	99.5	0.7	100.4	0.4	99.3	0.9	98.4	1.0	100.2	1.9	98.5	0.7	99.6	0.3	98.5	0.9

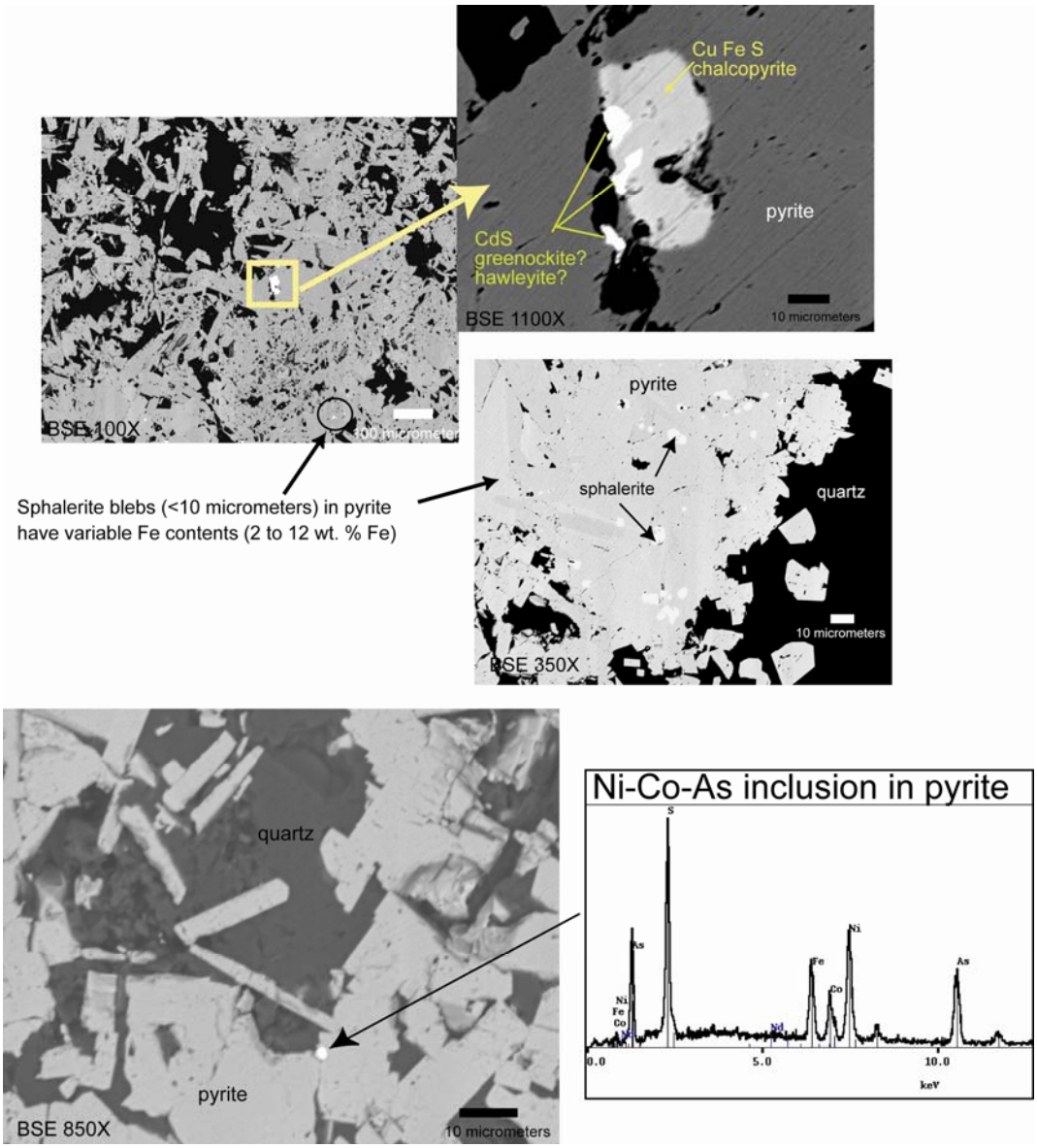

Figure 6. Mineral inclusions in pyrite. SEM images (backscattered-electron) showing inclusions of sphalerite, chalcopyrite, a cadmium sulfide mineral (greenockite or hawleyite), and a nickel-cobalt arsenate mineral in pyrite. As pyrite weathers, these minerals are subject to oxidation, especially by ferric iron.

EPMA, the composition is estimated: 29 wt. % Ni, 5 wt. % Co, 66 wt. % As. These inclusions were only identified in massive pyrite sampled from the center of the Skytop cut. The most common inclusions in vein pyrite are sphalerite and galena.

Clusters of dark reddish-brown sphalerite crystals (ruby jack) growing on quartz were found in excavated Skytop material (Fig. 7A). The dark color results from iron, which varies from about 3 to 10 wt. % (Table 3). Microprobe traverses across coarse crystals suggest that the crystals are zoned with respect to iron, which covaries with zinc (Fig. 7 B, C). Although many sphalerites are enriched in cadmium or manganese (as much as 4 to 5 wt. %), the Skytop sphalerites contain 0.05 wt. % Cd or less and negligible Mn. Other trace elements that were enriched in some sphalerites (Ge, In) were not detected in the Skytop or Schad samples by EPMA. Most of the sphalerite at Skytop occurs in an unusual texture as microscopic (<20 micrometers diameter) rounded blebs in pyrite (Fig. 6); bleb compositions generally are similar to coarse sphalerite but contain variable (0 to 0.6 wt. %) copper concentrations.

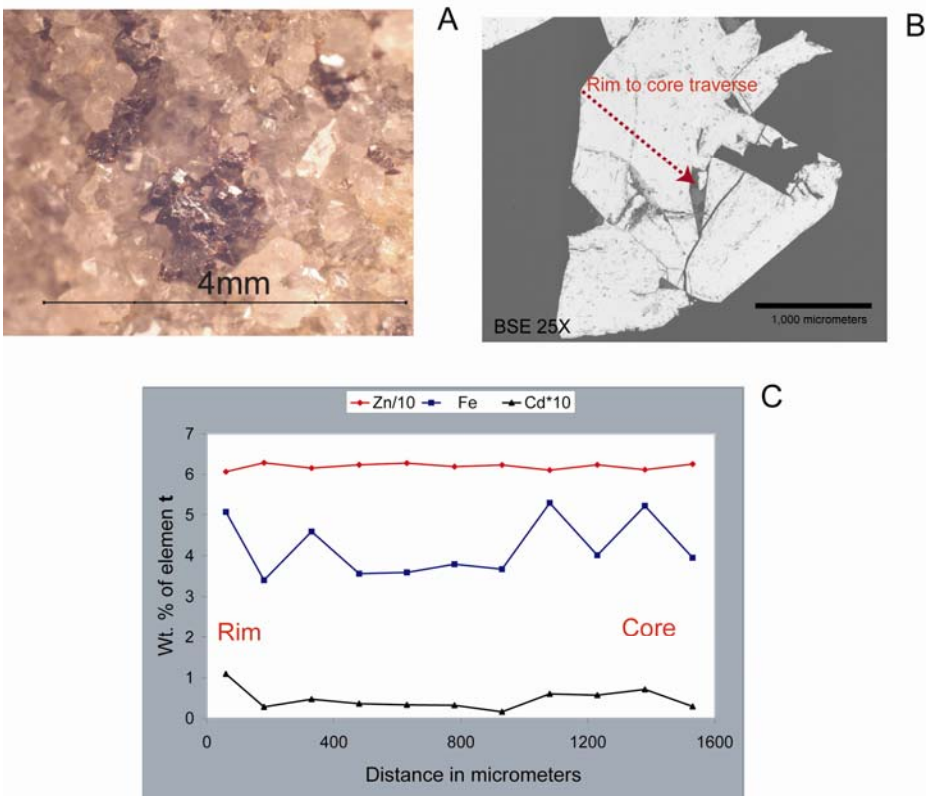

Figure 7. Sphalerite. A, Photograph showing mm-scale clots of reddish-brown sphalerite crystals on quartz. B, Backscattered-electron image (25 X) of a coarse sphalerite crystal. C, EPMA traverse across the crystal (b) showing rim to core variations in concentrations of Zn, Fe, and Cd.

Table 5. Sphalerite compositions determined by electron probe microanalysis (wt. %).

[N, number of analyses for each sample. Detection limits for all elements based on counting statistics range from < 0.01 to 0.03%]

Sample	**Arbogast pile**		**Skytop fault zone**		**Skytop fault zone**		**Schad 2**	
Mineral	Coarse crystals on quartz		Crystals (<30 µm) in pyrite		Blebs (<5 µm) in pyrite		Coarse crystals with galena	
N	16		4		7		5	
	Avg	SD	Avg	SD	Avg	SD	Avg	SD
Zn	62.01	0.82	55.88	0.24	57.17	3.84	62.89	2.46
Ni	0.00	0.00	0.00	0.00	0.00	0.00	0.00	0.00
Hg	0.00	0.00	0.00	0.00	0.00	0.00	0.00	0.00
S	33.39	0.24	34.74	0.36	34.95	0.70	33.46	0.30
Cu	0.02	0.03	0.10	0.05	0.21	0.25	0.06	0.05
Co	0.01	0.00	0.02	0.00	0.01	0.01	0.00	0.00
Ge	0.00	0.01	0.02	0.02	0.00	0.01	0.00	0.00
Pb	0.00	0.00	0.00	0.00	0.00	0.00	0.03	0.02
Fe	4.10	0.73	10.44	0.31	8.67	3.59	3.88	1.92
Te	0.00	0.01	0.01	0.00	0.00	0.01	0.00	0.00
As	0.00	0.00	0.00	0.00	0.00	0.00	0.00	0.00
Ag	0.00	0.00	0.00	0.00	0.00	0.00	0.00	0.00
Mn	0.03	0.01	0.03	0.00	0.03	0.02	0.01	0.00
Sb	0.00	0.01	0.01	0.01	0.00	0.00	0.00	0.00
Se	0.00	0.00	0.00	0.00	0.00	0.00	0.00	0.00
Cd	0.05	0.03	0.05	0.01	0.03	0.03	0.02	0.01
Total	99.61	0.38	101.29	0.30	101.09	0.72	100.36	0.89

Secondary minerals

Efflorescent sulfate salts have formed crusts on exposed rock surfaces along the Skytop cut (Fig. 8A), accumulated along pyrite veins and fractures where water collects (Fig. 8B), and precipitated from solution as pore waters or surface waters evaporate. Following a rain event, efflorescent salts may only be apparent in damp soil or under overhanging rock ledges that protect the highly soluble minerals from dissolving. On dry days, salts can quickly accumulate as an efflorescent "bloom" over large areas as the sulfate-rich solutions evaporate and progressively precipitate more material. As pyrite dissolves, the sandstone becomes more porous and friable, eventually disintegrating. The precipitation of efflorescent minerals can exacerbate the physical weathering. The molar volume of the salts is much larger than the molar volume of pyrite, so the formation of the salts within spaces previously occupied by pyrite and other pores can break the rock apart, analogous to the expansion of water during freezing that causes frost heaving (Fig. 8).

Efflorescent salts identified by XRD of Skytop samples include copiapite, melanterite, rozenite, halotrichite, and alunogen (Table 3). Different salts can form at different times, depending on the composition of the water evaporating to produce the salts, as well as on the temperature and relative humidity conditions. Melanterite typically is the first mineral to form. Pure melanterite is stable only at relative humidities >59% at 20 ^{o}C (Chou and others, 2002); at lower relative humidity melanterite dehydrates to rozenite. Melanterite can be colorless, white, green or blue-green; rozenite typically is white. Halotrichite is colorless and forms radiating bundles of crystals (Fig. 8C). Pyrite crystals associated with salts are pitted (Fig. 9A). Copiapite forms masses of yellow scales (Fig. 9B). EDS spectra show that copiapite and halotrichite at Skytop incorporate minor amounts of zinc (Fig. 9C). The salts are significant because they show that iron (both ferrous and ferric), aluminum, zinc, and sulfate are dissolved from the rocks at Skytop and are temporarily sequestered in these soluble minerals during dry periods. When it rains, the efflorescent salts readily dissolve and release their constituents to surface runoff or infiltrating waters. Iron oxide and iron oxyhydroxide minerals identified in the gossan, include hematite, goethite, and jarosite. Jarosite is indicative of acidic, high sulfate conditions.

Mineralogy of the Schad prospect

The small waste rock dump at the Schad prospect consists of loose pieces of quartzite. Some rocks contain coarse grains (>1 mm in diameter) and veinlets of reddish-brown sphalerite and galena. One sample contained a round clast of pyrite- cemented quartz grains within quartzite; a minor amount of pyrite is present in most samples but no pyrite veins were observed. The Fe-poor, Pb- and Zn-rich character of the Schad rocks relative to the Skytop samples is apparent in the bulk rock chemistry (Table 1). No efflorescent salts were noted at the Schad prospect. Microprobe data for six analyses of coarse galena from the Schad prospect averaged 88 wt. % Pb, 12 wt. % S with no anomalous trace-element concentrations at the level of detection. Sphalerites are similar to the Skytop sphalerites, but somewhat less Fe-rich (Table 5). In a spectrochemical study of trace elements in sphalerite and pyrite, Lenker (1962) included a sphalerite from Milesburg Gap (Schad prospect): 0.74 % Fe, 96 ppm Cu, 125 ppm Pb, 580 ppm Cd, 41 ppm Ge, and 62 ppm Ga. These data are consistent with our microprobe data. The Lenker study also included pyrites from Skytop and Milesburg. The Skytop pyrites had trace Ni (15 ppm) and Co (30 ppm) and 500 ppm Pb; the Milesburg pyrites had 3 ppm Ni, Pb (500 and 62 ppm), trace Ag, and Co was below detection limits. Galena and other mineral inclusions in pyrite are the likely source of the trace metals reported in pyrite. No arsenopyrite was observed in samples collected for this study. However, Howe's (1988) descriptions of the primary mineralogy of 18 samples of mineralized Tuscarora Formation from the dumps at the Schad adit included arsenopyrite as well as galena, sphalerite, pyrite, a Pb-Cu-Sb-As sulfosalt suggestive of bournonite, chalcopyrite, and minor pyrrhotite. Arsenopyrite occurs with pyrite in aggregates, as disseminations in sandstone, and as inclusions in sphalerite. Secondary minerals observed by Howe included native sulfur, smithsonite, anglesite , limonite, jarosite, melanterite, and anglesite or cerussite.

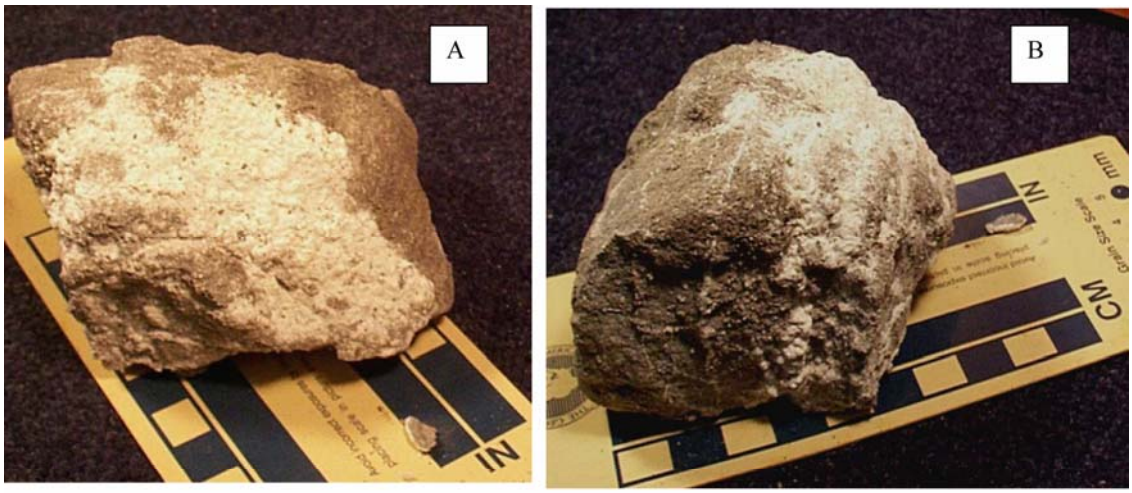

Mineral	Formula	Cell Volume (A^3)
Pyrite	FeS_2	159
Melanterite	$FeSO_4 \cdot 7H_2O$	977
Rozenite	$FeSO_4 \cdot 4H_2O$	641

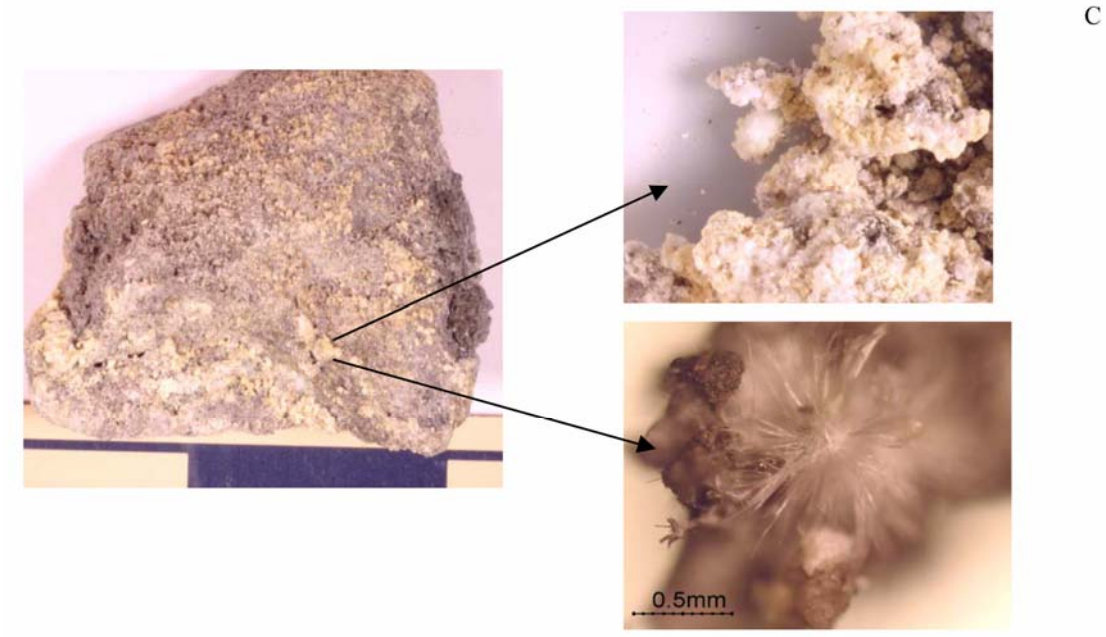

Figure 8. Efflorescent salts at Skytop, September, 2004. A, Efflorescent salt crust (mainly rozenite) on pyritic sandstone. B, Salts along fractures in sandstone. C, Sandstone disintegrating from effects of pyrite alteration. Clots of salts include white rozenite, yellow copiapite, and clear needles of halotrichite. Mineral formulas and cell volumes are noted in the table.

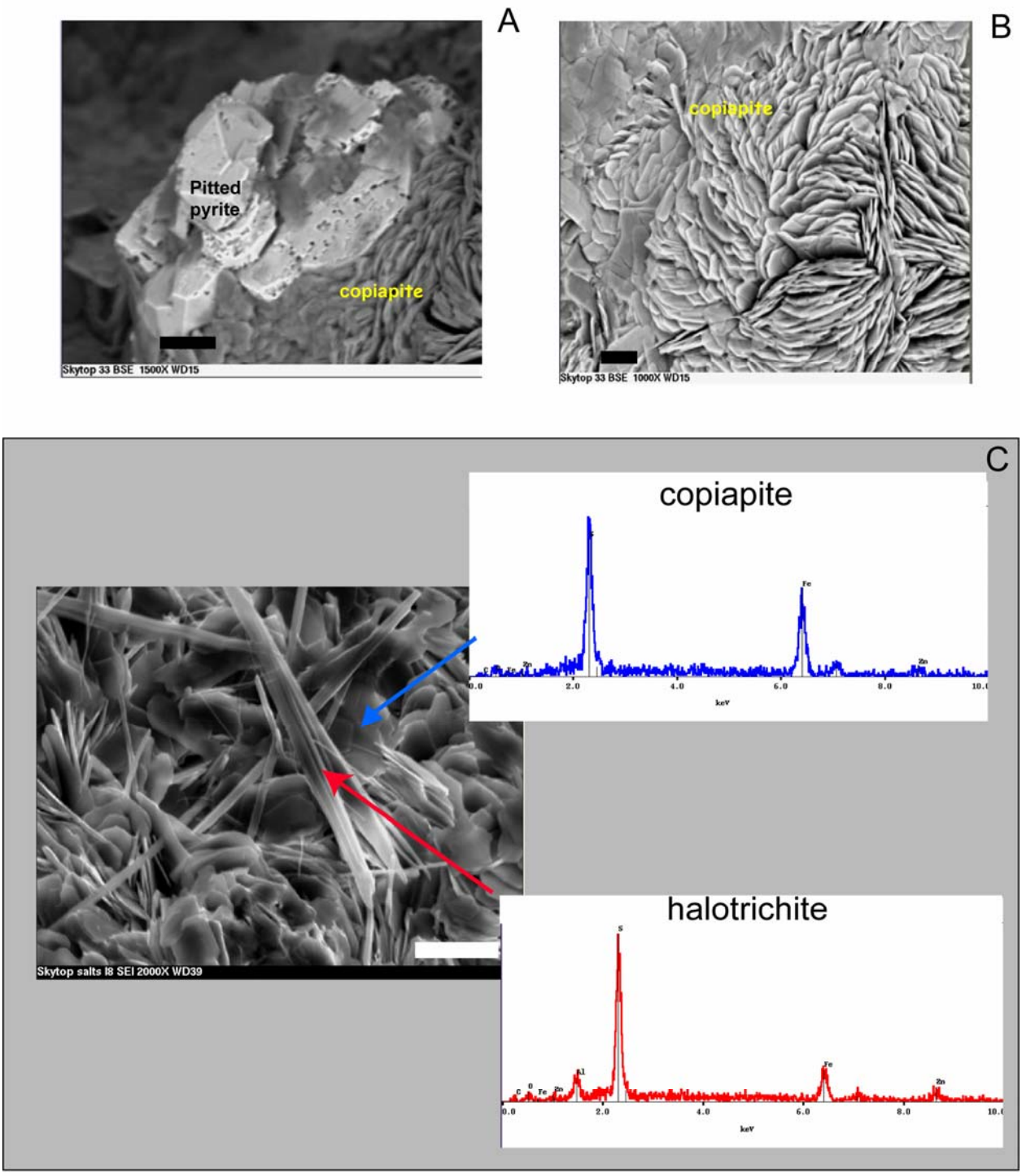

Figure 9. SEM studies on efflorescent salts. A, Backscattered-electron image of pitted pyrite associated with copiapite. B, Backscattered-electron image showing fish-scale texture of copiapite. C, Secondary-electron image of halotrichite needles on copiapite. EDS spectra show traces of zinc in both minerals. All scale bars are 10 micrometers long.

Skytop seep waters

Seep waters emanating from the Skytop fill and Arbogast aggregate stockpile in May of 2004 had very low pH (~2) and high specific conductance (>10,000 μS/cm) indicating high concentrations of dissolved solids. Chemical analysis of seep waters shows that they contain extreme concentrations of dissolved sulfate (>20,000 mg/L) as well as elevated concentrations of Al, As, Cu, Co, Fe, Ni, and Zn (Table 6). The low pH and extreme solute concentrations of sample Arbogast 2 probably reflect enrichment by evaporative concentration of the water in a small pool; other samples were flowing directly from the fill and had cooler temperatures reflecting their underground origin. The seeps result from surface-water infiltration and ground waters that may have migrated from bedrock and reacted with the pyritic fill material excavated from the Skytop cut. The seeps are not representative of groundwater at depth below the fill piles. The seep compositions provide the geochemical signature of the acid-rock drainage at Skytop. Seep waters are likely to be diluted with surface runoff before the waters reach Buffalo Run. However, seeps and puddles that develop in and at the base of fill piles may pose an attractive and potentially toxic water source for wildlife or domestic animals. All four seeps exceed U.S. EPA acute water-quality criteria for freshwater aquatic ecosystems for arsenic, copper, nickel, and zinc by factors of 10 to 1,000 (Table 6b). Thus, to reduce their potential toxicity, the seep waters would have to be significantly diluted, neutralized to remove metals, or both.

Table 6. Water chemistry data.

A. Water parameters, anion, and major cations.

[Skytop 2 and 3 are from Skytop fill flowing at 0.2 L/min. Arbogast samples represent a seep and small pool from the Arbogast aggregate pile.]

Sample	Units	Skytop 2	Skytop 3	Arbogast 1	Arbogast 2
Date		5/11/04	5/11/04	5/11/04	5/11/04
pH		2.3	2.2	2.1	2.0
Eh		518	500	469	470
SC	μS/cm	11,650	14,150	28,300	30,300
		Anions by ion chromatography			
F	mg/L	1.42	1.32	13.5	15.5
Cl	mg/L	33.2	17.2	60.2	50.4
Br	mg/L	<3.00	<3.00	<12.0	<12.0
NO_3 (as N)	mg/L	3.30	3.61	<4.00	<4.00
PO_4 (as P)	mg/L	<2.00	<2.00	<8.00	<8.00
SO_4	mg/L	20,900	24,100	86,500	97,600
		Major cations by ICP-OES			
Al	mg/L	1,190	1,410	5,660	6,430
Ca	mg/L	690	605	672	741
Fe	mg/L	1,850	2,650	15,400	18,200
Mg	mg/L	491	389	2,370	2,660
Mn	mg/L	44	48	400	444
Na	mg/L	103	89	345	384
Si	mg/L	98	102	154	175

B. Trace elements (µg/L)

[Analysis by ICP-MS; Ag, Au, Bi, K, Hg, Mo, Os, Re, Sn were below detection limits; [1], Analysis by ICP-OES; U.S. EPA, National recommended water quality criteria for priority toxic pollutants for freshwater aquatic life (U.S. EPA, 2004). CMC, criteria maximum concentration; CCC, criterion continuous concentration for assumed hardness of 100 mg/L $CaCO_3$]

Sample	Skytop 2	Skytop 3	Arbogast 1	Arbogast 2	EPA CMC	EPA CCC
As	1,170	1,520	24,900	29,300	340	150
Ba	14	13	<10	10		
Be	62	66	396	453		
Br	<300	<300	564	410		
Cd	193	242	1,690	1,950	2	0.25
Cd[1]	288	362	2,650	3,060	2	0.25
Ce	1,580	1,410	2,560	2,930		
Co	4,050	4,130	34,400	41,600		
Cr	879	976	4,830	5,460		
Cs	1.1	0.7	0.3	0.3		
Cu[1]	6,240	7,070	118,000	135,000	13	9
Dy	332	392	1,780	2,090		
Er	186	215	1,020	1,150		
Eu	101	119	506	576		
Ga	68	86	228	256		
Gd	426	509	2,020	2,330		
Ge	7	7	23	25		
Hf	7.9	9.2	39.8	42.9		
Ho	65.4	76.0	352	402		
I	144	117	577	806		
In	3.6	4.2	20.8	24		
La	444	502	589	661		
Li	1,050	1,130	6,150	6,760		
Lu	21.2	24.2	118	131		
Nb	<0.5	0.5	1.9	2.3		
Nd	1,400	1,590	3,900	4,410		
Ni[1]	6,870	8,060	81,000	91,000	470	52
Pb	10	4	3	5	65	2.5
Pd	<1	<1	2	<1		
Pr	271	307	579	658		
Rb	13.4	11.7	5.7	7.3		
Ru	<1	<1	2	2		
Sb	<1	<1	4	5		
Sc	630	613	2,930	3,210		
Se	94	82	360	401		
Sm	464	530	2,000	2,290		
Sr	661	717	400	459		
Ta	0.9	0.9	4.2	4.6		
Tb	63	75.3	333	380		
Te	<1	<1	8	9		
Th	435	426	1,160	1,340		
Ti	80	81	1,070	1,180		
Tl	0.6	0.2	0.1	0.2		
Tm	23.6	27.5	133	152		
U	163	174	1,060	1,220		
V	160	223	3,890	4,260		
W	4	4	17	19		
Y	1,880	2,130	9,140	10,500		
Yb	150	172	852	966		
Zn[1]	132,000	169,000	973,000	1,120,000	120	120
Zr	54	52	152	171		

Discussion

Sources of acid-rock drainage at Skytop

Weathering of pyrite

There are thousands of known minerals, but only three are the primary cause acid-rock drainage: pyrite (FeS_2), marcasite (another form of FeS_2), and pyrrhotite ($Fe_{1-x}S$, where x=0 to 0.17). All three minerals are present at Skytop. The weathering of pyrite starts with exposure of pyrite to oxygen (in air) and water (rain, snow, humid air). Pyrite is less reactive if submerged in water. In general, it is the exposure of pyritic rocks to repeated wet/dry cycles and the action of bacteria present at the earth surface that generates acid drainage. Some of the generalized chemical reactions used to describe the cycle of pyrite/marcasite oxidation are described below. The complex details of the oxidation process are described by Rimstidt and Vaughan (2003).

Initial reaction:

$$FeS_2 + 3.5\ O_2 + H_2O \rightarrow Fe^{2+} + 2\ SO_4^{2-} + 2H^+$$

Ferrous iron released from initial pyrite/marcasite oxidation is oxidized to ferric iron by bacteria that are ubiquitous in the environment. There are several aerobic autotrophic bacteria that can obtain energy from oxidation of sulfide minerals, such as *Acidithiobacillus ferroxidans* (Gould and Kapoor, 2003). The oxidation of ferrous iron by bacteria is much faster than abiotic oxidation (Singer and Stumm, 1970). The oxidation of ferrous iron is described by the reaction:

$$Fe^{2+} + 0.25\ O_2 + H^+ \rightarrow 0.5\ H_2O + Fe^{3+}$$

Once formed, ferric iron is a powerful oxidant that can attack pyrite and other minerals and release significant amounts of ferrous iron and acidity that can further propagate the cycle of pyrite oxidation:

$$14\ Fe^{3+} + FeS_2 + 8\ H_2O \rightarrow 15\ Fe^{2+} + 2\ SO_4^{2-} + 16H^+$$

Note that the initial reaction produced 2 moles of acid (H^+), but the propogation reaction with ferric iron as the oxidizing agent produces 16 moles of acid. Sulfide minerals that have metal/sulfur ratios = 1 such as sphalerite (ZnS) and galena (PbS) are not strongly oxidized by oxygen, but are affected when ferric iron is the oxidant (Plumlee, 1999):

$$ZnS + 8\ Fe^{3+} + 4\ H_2O \rightarrow Zn^{2+} + 8Fe^{2+} + SO_4^{2-} + 8H^+$$

Unless the acid (H^+) generated by these reactions is counteracted by a neutralizing agent, a serious acid-drainage problem can develop. Most metals that behave as cations are more mobile at low pH. If metals such as zinc and copper are available, they will tend to remain in solution as dissolved species at low pH. The products of the chemical reactions that dissolve pyrite and other sulfide minerals can (1) remain as dissolved constituents, (2) form secondary minerals such as efflorescent sulfate salts due to evaporation, (3) undergo hydrolysis reactions and precipitate as new minerals such as iron oxyhydroxides, and (4) propogate the weathering cycle as reactants. Because ferrous iron and sulfate are present as aqueous species (aq) as products of pyrite weathering, melanterite commonly forms first as the solutions evaporate (Nordstrom and Alpers, 1999). Oxidation of ferrous to ferric iron can lead to formation of mixed valence salts like copiapite. Other dissolved species can be incorporated in salts as major or trace constituents. For example, the formation of solid halotrichite from aqueous species can be described by the reaction:

$$Fe^{2+}_{(aq)} + 4\ SO_4^{2-}{}_{(aq)} + 2Al^{3+}_{(aq)} + 22\ H_2O \rightarrow\ FeAl_2(SO_4)_4 \bullet 22\ H_2O_{(s)}$$

Melanterite, rozenite, copiapite, and halotrichite are all soluble in water; once formed, they only persist if conditions remain relatively dry or if they are protected in some way. Thus, they may or may not be apparent at a given site on a given day depending on weather conditions. The salts are important to recognize because they store metals and acidity that can subsequently degrade water quality. Studies have shown that dissolution of salt accumulations along stream banks during a rainstorm temporarily lowers pH and increases metal loads in streams (Dagenhart, 1980). Such water-quality impacts can have catastrophic effects on aquatic ecosystems, such as fish kills, and can complicate efforts to treat acid drainage. Snow melt can also flush salts leading to pulses of contaminated water flowing into streams (Hammarstrom and others, 2004).

Oxidation of ferrous iron (shown above) and subsequent hydrolysis can lead to the formation of goethite and additional acid:

$$Fe^{3+}{}_{(aq)} + 2H_2O \rightarrow FeOOH + 3H^+$$

Goethite is the most stable ferric oxide mineral commonly found in surficial deposits (Bigham, 1994). A variety of other ferric iron oxyhydroxide minerals, such as ferrihydrite, or iron hydroxysulfate minerals, such as schwertmannite, may form as precursors to goethite depending on the local chemical environment (Bigham and others, 1996; Yu and others, 1999). These minerals, collectively referred to as ochres, appear as rusty spots around pyrite or as crusts on completely weathered pyritic rock surfaces (e.g., gossan in Fig. 4c), in soils developing on weathering pyritic rock, and as muds that precipitate in puddles and streams affected by acid-rock drainage.

Other factors that affect ARD

Although limestone is locally abundant in central Pennsylvania (Fig. 1), the rocks at Skytop are sandstones, quartzites, and shales that lack any inherent acid-neutralizing capacity. Calcite (limestone) is the most widely available and effective naturally occurring neutralizing agent in the eastern United States. Some common rock-forming silicate minerals also have acid-neutralizing capacity, but typically react at a rate too slow to offset the rate of acid generation (Jambor, 2003). Streams that flow through limestone may attain enough alkalinity to buffer the effects of acidic influent. However, the acid-neutralizing capacity of these streams may not be as large as the potential acid-loading rate. Studies are ongoing to evaluate various potential effects and capacities for mixing of acidic influent with the water from Buffalo Run and North Bald Eagle Creek (DeAngelo, 2004, written commun.).

Water quality and implications for remediation

Most acid-drainage problems in Pennsylvania are associated with coal-mine drainage where concentrations of Fe, Al, Mn, and acidity can exceed water-quality standards. However, the situation at Skytop is different because of the more complex mineralogy that includes sphalerite (ZnS), galena (PbS) and other minerals in addition to pyrite (FeS_2). Seep analyses indicate that dissolved As, Cu, Ni, and Zn are elevated in addition to Fe and Al. In discussions of the geochemical signatures of waters associated with metal mines, it is useful to display the water chemistry on plots known as Ficklin diagrams to show variations in total dissolved base-metal concentrations (Zn+Cu+Cd+Pb+Co+Ni) as a function of pH (Plumlee and others, 1999). Figure 10 shows the Skytop seep waters (Table 6) on a Ficklin diagram, along with other Skytop seep data from March and April 2004 (PADEP, unpublished data), the soil leachate, Pennsylvania coal-mine drainage (Cravotta and others, 2001; Cravotta and Kirby, 2004; Cravotta, 2005), and waters associated with the Valzinco mine in central Virginia (Hammarstrom and others, 2004, unpublished data). The diagram is divided into regions of low- to extreme-metal concentrations as well as into pH regions. The arrow indicates the general trend that waters associated with mineral deposits follow as pyrite content (or evaporation) increases or carbonate-mineral content decreases. All of the Skytop waters plot in the acid or high-acid fields; total base-metal concentrations range from high to extreme. Natural water from the Tuscarora Formation (background) plots at a pH of 5.5 with an extremely low concentration of base metals. Pennsylvania coal-mine drainage straddles a large field, from near-neutral to high-acid, low-metal to high-metal, with metals increasing as pH decreases. The composition of the soil leachate lies within the field defined by the seep waters. Most of the Skytop waters are worse (in terms of acid and metals) than even the worst coal-mine drainage. The Skytop seep waters are more comparable to acid drainage associated with metal mines (Fig. 10). Surface waters (seeps and stream) associated with the Valzinco mine (Seal and others, 2002) are shown for reference. Valzinco is an abandoned zinc-lead mine that exploited a massive sulfide deposit hosted by carbonate-poor volcanic rocks, where surface runoff and seeps from pyritic mine tailings contaminated a stream. Long-term water-quality monitoring showed that metal concentrations (mainly zinc) and low pH in the stream at Valzinco peaked during summer base-flow conditions, partially due to evaporative concentration. Like the Skytop cut, the Valzinco mine tailings developed intermittent blooms of efflorescent sulfate salts that were periodically flushed. The State of Virginia reclaimed the mine site in 2000 using several approaches to remove the pyritic material from continued exposure to air and water (Sobeck, 2000).

The geochemical signature of the Skytop seeps reflects the presence of observed primary and secondary minerals, but not necessarily their abundances. Oxidative weathering of pyrite and marcasite accounts for the low pH and elevated iron and sulfate concentrations in the seep waters. Marcasite and pyrite oxidize faster than the other sulfide minerals at Skytop and promote the acidic weathering of associated minerals. The relative rates of weathering of iron sulfides and other minerals depend on a number of factors, including the mineral textures and the exposed surface area and the solution pH and concentrations of Fe^{3+}. The unusual whisker forms of some pyrites at Skytop provide larger surface area for reactions with air, water, and microbes compared to typical cubic forms. Excavation and crushing of the sandstone during construction increased the exposed surface area and enhanced the weathering of the

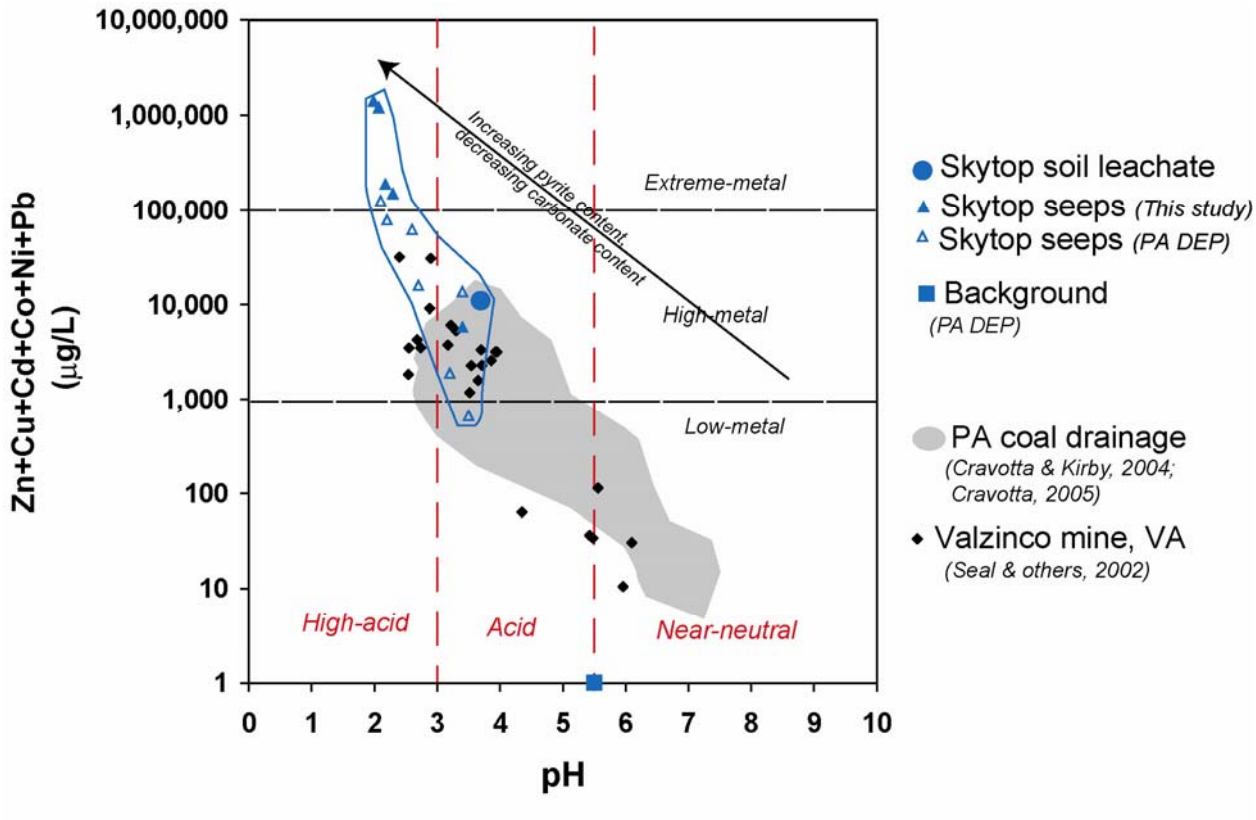

Figure 10. Ficklin diagram for Skytop seep waters, Skytop soil leachate, waters associated with coal-mine drainage in Pennsylvania (Cravotta and others, 2001; Cravotta and Kirby, 2004; Cravotta, 2005), and waters associated with the Valzinco mine in central Virginia (Seal and others, 2002).

pyrite and other sulfides in the fill and crushed rock piles. As the pyrite dissolves, inclusions of sphalerite (Zn source) and chalcopyrite (Cu source) in pyrite are subject to weathering and release Zn and Cu into solution. Sphalerite is much more abundant than galena (Pb source) at Skytop; Zn is also greater than Pb in Skytop seep waters. Although lead constitutes ~1 wt. % of some of the pyritic rocks (Table 1b), dissolved lead concentrations in the seeps are less than 10 µg/L (Table 6b). The low concentrations of dissolved lead are consistent with potential solubility control by sulfate minerals at low pH; however, computed saturation indices for the samples collected in May 2004 indicate undersaturation with anglesite (Table 7). Sphalerite and greenockite/hawleyite are the sources of the dissolved Cd. Identification of skutterudite(?) inclusions in pyrite establishes a possible source for the elevated concentrations of Ni, Co, and As in the Skytop seeps. These elements also may be present in trace amounts in pyrite or in other minerals that have not yet been identified. Howe (1988) described arsenopyrite in a number of samples from the Schad prospect. Arsenopyrite may also be present at Skytop, but has not yet been identified. Elevated concentrations of dissolved Al and Si reflect acid dissolution of clay and other aluminosilicate minerals in the host rocks. Although the Bald Eagle Formation is composed predominantly of quartz, clasts of shale are present in the sandstone exposed in the cut and the east end of the cut exposes shale of the Reedsville Formation Shale is an aluminum-rich rock that may represent the source of the elevated aluminum concentrations in the Skytop seeps.

Water sampled from a puddle at the base of a fill pile at Skytop evaporated completely to form a mixture of copiapite and alunogen. The seepage samples collected in May 2004 were saturated with respect to amorphous silica, gypsum, goethite, allophane, jurbanite, and barite (Table 7). The samples were close to saturation with melanterite ($-1 < SI < 0$), but were undersaturated with jarosite, anglesite, and various other sulfate or hydroxide minerals (Table 7). A pH value of 2.0 for the most concentrated seepage samples (Table 6a, Arbogast 2) indicates possible pH buffering due to equilibrium between sulfate and bisulfate ($SO_4^{-2} + H^+ = HSO_4^-$; $K = 10^{-1.99}$). With continued evaporation of this sample, and possibly other Skytop seepage samples, dissolved solute concentrations would increase, but H^+ ($= 10^{-pH}$) would not be expected to increase to the same extent because of the formation of bisulfate. Bisulfate formation also would decrease the availability or activity of sulfate ions. Hence, saturation with sulfate minerals would be less favorable for pH values < 2 than for higher pH solutions containing the same concentrations of solutes. Although thermodynamic data are not available for many of the sulfate minerals observed at Skytop, geochemical modeling of evaporation, mineral precipitation, and dissolution, and mixing of the acidic

Table 7. Mineral saturation indices computed for seepage samples collected at Skytop, May 2004.

[Computations performed using WATEQ4F version 2.63 of Ball and Nordstrom (1991)]

Log AP/K for Minerals	Mineral Formula	Skytop2	Skytop3	Arbogast1	Arbogast2
Chalcedony	SiO_2	1.12	1.26	1.36	1.43
SiO_2(amorphous)	SiO_2	0.28	0.39	0.54	0.61
Gypsum	$CaSO_4 \bullet 2H_2O$	0.18	0.16	0.28	0.34
Epsomite	$MgSO_4 \bullet 7H_2O$	-2.22	-2.18	-1.50	-1.44
Gibbsite	$Al(OH)_3$	-4.25	-5.14	-4.21	-4.38
Allophane(amorphous)	$[Al(OH)_3]_{(1-x)}[SiO_2]_{(x)}$	-0.15	-0.03	0.32	0.46
Alunite	$KAl_3(SO_4)_2(OH)_6$	-3.31	-5.04	-2.31	-2.55
Jurbanite	$AlOHSO_4$	0.56	0.54	0.98	0.97
Goethite	FeOOH	1.46	0.59	0.99	0.85
Ferrihydrite	$Fe(OH)_3$	-4.48	-4.99	-5.16	-5.32
Strengite	$FePO_4 \bullet 2H_2O$	0.03	-0.62	-0.40	-0.54
Jarosite	$KFe_3(SO_4)_2(OH)_6$	-3.84	-6.01	-4.10	-4.28
Melanterite	$FeSO_4 \bullet 7H_2O$	-1.92	-1.58	-0.91	-0.83
$MnHPO_4$	$MnHPO_4$	-0.76	-0.97	-0.12	-0.20
Barite	$BaSO_4$	0.34	0.53	-	0.38
Celestite	$SrSO_4$	-1.11	-1.05	-1.19	-1.11
Goslarite	$ZnSO_4 \bullet 7H_2O$	-3.50	-3.28	-2.58	-2.50
Anglesite	$PbSO_4$	-2.47	-2.81	-2.91	-2.68
Hinsdalite	$PbAl_3PO_4SO_4(OH)_6$	-23.19	-24.62	-24.23	-24.53
Morenosite	$NiSO_4 \bullet 7H_2O$	-4.22	-4.03	-3.01	-2.94
$AlAsO_4 \bullet 2H_2O$	$AlAsO_4 \bullet 2H_2O$	-6.63	-6.87	-5.36	-5.43
Scorodite	$FeAsO_4 \bullet 2H_2O$	-5.59	-6.02	-4.72	-4.76
$CdSO_4 \bullet 2.67H_2O$	$CdSO_4 \bullet 2.67H_2O$	-6.53	-6.52	-5.41	-5.32
Chalcanthite	$CuSO_4 \bullet 5H_2O$	-4.02	-3.88	-2.57	-2.49

seepage with higher pH solutions could be helpful to evaluate secondary mineral precipitation and other possible controls on the transport of metals from Skytop.

Relative to average elemental compositions of dissolved constituents in surface waters worldwide (Martin and Whitfield, 1983), the Skytop seeps contain anomalously high concentrations of transition metals, rare-earth elements, and lithium (Table 6b). The rare-earth elements are not present in elevated concentrations in the pyritic rocks analyzed (Table 3); however, rare-earth elements are present in phosphate minerals identified at Skytop and could be present in other minerals. Comparison of Skytop seep data with regional ground waters and monitoring well data from Skytop could elucidate the seep chemistry. Anthropogenic sources of elevated trace-element concentrations cannot be ruled out. Neutralizing materials applied to the fill could contribute to the chemical signature of the seeps. For example, Smith (1977) noted that fluorine anomalies detected in water wells in Bald Eagle Valley could result from fluorite (in brecciated Tonoloway limestone along Interstate 80 at Curtin Gap north of Skytop) related to regional Zn-Pb mineralization; alternatively, the anomalies could result from the use of phosphate fertilizers. Cravotta (1986) also noted fluorine, strontium, and barium anomalies in domestic water wells screened within a zone of potential Zn-Pb mineralization in Sinking Valley, Blair County, as well as nitrate anomalies associated with dairy farming activities. Wood (1980) reported partial chemical analyses for groundwater from wells and springs in several aquifers in Centre County; highest concentrations of sulfate (79 mg/L) were reported for waters from Silurian rocks (Tuscarora Formation and others).

In the fall of 2004 (after our water sampling), black plastic was installed over the Skytop fill and other fill areas as a stopgap measure to minimize infiltration through the crushed rock while a long-term solution to the problem is sought. Meanwhile, seep waters and surface runoff from the cut face and fills are collected from discharge locations and treated on-site. Nevertheless, some mineralized solutions could continue to infiltrate

through the roadcut face and from within the covered fills. Information about the geochemical signature of the acidic drainage is essential for the development of appropriate remediation strategies and for the detection of the potential for offsite migration of contaminants. Although some methods of treatment for coal- and metal-mine drainage could be applicable, they may not be entirely adequate for the suite of contaminants present at Skytop. Although the covers may reduce direct infiltration of water into fill piles, moist air will not be excluded. Oxygen and moisture in the air could continue to promote oxidation of pyrite in the covered fill areas, and salts could continue to form beneath the plastic as well as on exposed pyritic materials. Seasonal as well as short-term climate variations are likely to affect surface runoff water quality due to rapid dissolution of accumulated salts. Surface runoff and ground-water quality should be monitored over a long enough period of time to include seasonal variations for adequate design of a long-term solution to the acid-rock drainage problem at Skytop.

Is Skytop unique?

Acid-rock drainage develops in pyritic rocks exposed during construction projects in other places in the eastern U.S. There are several regionally-extensive formations that are known from geologic mapping to be pyritic. These include the Anakeesta Formation of the Great Smoky Group that crops out in the Great Smoky Mountains and other parts of the southeast, rocks of the Meguma Group in Nova Scotia (Zentelli and Fox, 1997), and rocks in the Coastal Plain, Blue Ridge, Piedmont, and Valley and Ridge physiographic provinces in Virginia.

Highway and powerline construction through rocks of the Anakeesta Formation poses acid-rock drainage problems (Byerly, 1996; Schaeffer and Clawson, 1996). Near the southeast corner of Great Smoky Mountains National Park, a highway project was halted in part because of problems caused by acid-generating materials leading to the designation "Road-to Nowhere" for the incompleted road along the north shore of Fontana Lake (Southern Appalachian Forest Coalition, 2003). Similar problems were encountered at Newfound Gap in Great Smoky Mountains National Park (Trumpf and others, 1979; Hammarstrom and others, 2003b), during construction of the Cherohala Skyway, a 50-mile long National Scenic Byway that connects Robbinsville, North Carolina and Tellico Plains, Tennessee (Tingle, 1995), and in construction of the 1994 Olympic whitewater center along the Ocoee River in Tennessee (Byerly, 1994).

In an evaluation of sulfidic materials in Virginia highway corridors, Orndorff (2001) developed a state-wide sulfide hazard rating map based on geology to assist in the pre-design phase of construction projects. In addition to water-quality threats, Orndorff discussed problems with fill stability, integrity of building materials, and vegetation management that occur with weathering of sulfidic rocks because of heaving and development of acid-sulfate soils.

Acid-mine drainage is a severe problem at many coal- and metal- mines in the eastern U.S. The State of Pennsylvania has developed special handling techniques to prevent or minimize acid-mine drainage at surface mines (Perry and others, 1998). Guidelines have been established for handling excavated acid-producing materials in highway construction (Byerly, 1990). Nevertheless, the extent of the acid-producing material at Skytop was unanticipated and plans were not developed in advance for the handling of the pyritic materials. The Skytop highway construction exposed a mineral deposit that had not been known to exist. The Bald Eagle Formation and other rocks exposed in the cut are present in other places where they are not pyritic. Most of the zinc-lead deposits in Pennsylvania are in carbonate rocks rather than sandstones. Because of the structural geology that allowed mineralizing fluids to infiltrate the rock, the Bald Eagle Formation at Skytop became the host rock for the mineral deposit. Pyrite veins and disseminated pyrite commonly are associated with mineral deposits, most of which are never developed as mines because of their low grade or tonnages or other factors that make them uneconomic. Recognition of indicators of mineral deposits during planning stages of construction projects might prevent other Skytop situations by allowing planners to reroute roads or better anticipate the occurrence of acid-producing materials. In retrospect, indicators that were present at Skytop included the gossan, reported ore-mineral occurrences, anomalous concentrations of metals in stream sediments and surface waters, and distributions of structurally-controlled mineral occurrences and prospects along Bald Eagle Mountain.

Conclusions

The acid-rock drainage at the Skytop I-99 roadcut is caused by the exposure and rapid weathering of pyrite associated with a previously unknown zinc-lead sulfide deposit. Exposure of fresh pyrite surfaces to air and water

initiated a complex series of chemical and microbial reactions that created acidic conditions and dissolved a variety of minerals in the rock, mobilizing trace metals. The primary minerals in the rock and secondary minerals that form through the weathering process affect the chemistry of the acid-rock drainage. In addition to pyrite, rocks exposed at Skytop contain sphalerite and traces of galena and other minerals that contain zinc, lead, nickel, cobalt, cadmium, and arsenic. These elements are concentrated in seeps and puddles at the Skytop site and greatly exceed criteria for protection of fresh-water aquatic organisms. In addition the seeps and soil leachate contain elevated concentrations of dissolved iron, aluminum, and sulfate. Highly soluble sulfate minerals crystallize on the cut face and fill piles immobilizing the metals when these waters evaporate; however, during rain events, these minerals readily dissolve releasing the stored acidity and metals to runoff and infiltrating ground water. The cycle of salt formation and dissolution will contribute to acid-drainage from the site as long as pyritic material remains exposed to air, water, or moist air.

Skytop poses a reclamation challenge because of the volume and distribution of pyritic material, the relative lack of neutralizing minerals in the host rock, and the low pH and complex chemistry of the acid drainage. The same processes of oxidative weathering of pyrite are responsible for the acid drainage from coal mines in Pennsylvania and elsewhere plus other highway construction sites. The situation at Skytop, however, is more extreme and comparable to environmental problems that develop at historic metal mines where pyritic materials were not handled with concerns for acid formation and release of potentially toxic metals to the environment.

Acknowledgements

This study was conducted in cooperation with the Pennsylvania Department of Environmental Protection. Dr. Andrew Sicree and Dr. David Gold of Pennsylvania State University kindly organized an introductory field trip to Skytop and Milesburg Gap in June 2004, along with colleagues Dr. Art Rose (Penn State), Dr. Ryan Mathur (Juniata College), and Dr. Allen Heyl (USGS). Dr. Stephen S. Howe of the State University of New York at Albany kindly shared his expertise on the central Pennsylvania lead-zinc deposits. PennDOT personnel, especially Tom McNally, provided site access and site tours. Nadine M. Piatak, USGS (Reston) conducted the leach test. Monique Adams, USGS (Denver) and Paul Briggs, USGS (Denver) analyzed the soil leachate chemistry. The authors thank Dr. Hubert Barnes and Dr. David Gold for the opportunity to participate in the 2004 Conference on Principles of Acid Pollution Control Along Highways. The U.S. Geological Survey Mineral Resources Program provided funding for this research. This report benefited from reviews by Dr. Robert R. Seal, II, Nadine M. Piatak, and Dr. Avery Drake.

Literature Cited

Ball, J.W., and Nordstrom, D.K., 1991, User's manual for WATEQ4F with revised data base: U.S. Geological Survey Open-File Report 91-183, 189 p.

Berg, T.M., Edmunds, W.E., Geyer, A.R., and others, compilers, 1980, Geologic map of Pennsylvania: Pennsylvania Geological Survey, 4th series, Map 1, scale: 1:250,000.

Berg, T.M., and Dodge, C.M., 1981, Atlas of preliminary geologic quadrangle maps of Pennsylvania: Pennsylvania Geological Survey, 4th Series, Map 61: Accessed 1/21/05 at: http://www.dcnr.state.pa.us/topogeo/map61/61intro.aspx

Bigham, J.M., 1994, Mineralogy of ochre deposits formed by sulfide oxidation, *in* Jambor, J.L., and Blowes, D.W., eds., 1994, The environmental geochemistry of sulfide mine-wastes: Mineralogical Association of Canada, Short Course Handbook, v. 22, p. 103-132.

Bigham, J.M., Schwertmann, U., Traina, S.J., Winland, R.L., and Wolf, M., 1996, Schwertmannite and the chemical modeling of iron in acid sulfate waters: Geochimica et Cosmochimica Acta, v. 60, p. 2111-2121.

Butts, C. and Moore, E.S., 1936, Geology and mineral resources of the Bellefonte quadrangle, Pennsylvania: U.S. Geological Survey Bulletin 855, 111p.

Byerly, D.W., 1990, Guidelines for handling excavated acid-producing materials: U.S. Department of Transportation, Federal Highway Administration, DOT FHWA-DF-89-001, Washington, D.C., 81 p.

Byerly , D.W., 1994, Characterization of rocks for the proposed Ocoee Olympic Whitewater Venue, Polk County, Tennessee. Report of Investigation, *in* USDA Forest Service Final EIS, 1996 Olympic whitewater slalom venue, Ocoee River, Polk Co, TN, Ocoee Ranger District, Cherokee National Forest: Management Bulletin R8-MB 68-A, p. G-5-1 – G-5-10.

Byerly, D.W., 1996, Handling acid-producing material during construction: Environmental and Engineering Geoscience, v. II, no. 1, p. 49-57.

Chou, I.M., Seal, R.R. II, and Hemingway, B.S., 2002, Determination of melanterite-rozenite and chalcanthite-bonatitte equilibria by humidity measurements at 0.1 MPa: American Mineralogist v. 87, p. 108-114.

Commonwealth of Pennsylvania, 1998, Chapter 87, Surface mining of coal. Pennsylvania Code, Title 25. Environmental Protection: Harrisburg, Pennsylvania, Commonwealth of Pennsylvania, p. 87.1-87.122.

Commonwealth of Pennsylvania, 2002, Chapter 93, Water Quality Standards. Pennsylvania Code, Title 25. Environmental Protection: Harrisburg, Pennsylvania, Commonwealth of Pennsylvania, p. 93.1-93.226.

Commonwealth of Pennsylvania, 2005, Chapter 16, Water Quality Toxics Management Strategy—Statement of Policy, Pennsylvania Code, Title 25. Environmental Protection: Harrisburg, Pennsylvania, Commonwealth of Pennsylvania, Chapter 16. Accessed 3/22/05 at:
http://www.pacode.com/secure/data/025/chapter16/chap16toc.html#16.24

Cravotta, C.A., III, 1986, Spatial and temporal variations of ground-water chemistry in the vicinity of carbonate-hosted zinc-lead occurrences, Sinking Valley, Blair County, Pennsylvania: Pennsylvania State University, M.S. thesis, 405 p.

Cravotta, C.A., III, 2005, Effects of abandoned coal-mine drainage on streamflow and water quality in the Mahanoy Creek Basin, Schuylkill, Columbia, and Northumberland Counties, Pennsylvania, 2001: U.S. Geological Survey Scientific Investigations Report 2004-5291, 60 p.

Cravotta, C.A., III, and Bilger, M.D., 2001, Water-quality trends for a stream draining the Southern Anthracite Field, Pennsylvania: Geochemistry - Exploration, Environment, Analysis, v.1, p. 33-50.

Cravotta, C.A., III, and Kirby, C.S., 2004, Effects of abandoned coal-mine drainage on streamflow and water quality in the Shamokin Creek Basin, Northumberland and Columbia Counties, Pennsylvania, 1999-2001: U.S. Geological Survey Water-Resources Investigations Report 03-4311, 53 p.

Cravotta, C.A., III, Breen, K.J., and Seal, R., 2001, Arsenic is ubiquitous but not elevated in abandoned coal-mine discharges in Pennsylvania (abs.), in U.S. Geological Survey Arsenic Workshop, February 2001: U.S. Geological Survey, http://wwwbrr.cr.usgs.gov/Arsenic/FinalAbsPDF/cravatta.pdf.

Dagenhart, T.V., Jr., 1980, The acid mine drainage of Contrary Creek, Louisa County, Virginia - Factors causing variations in stream water chemistry: University of Virginia, M.S. Thesis, 215 p.

Detrie, T.A., Mutti, L.J., and Mathur, R. 2005, Quartz sulfide mineralization of the Bald Eagle Formation of Skytop Mountain, near State College, Pennsylvania: Geological Society of America Abstracts with Programs, v. 37, no. 1, p. 61.

Fortescue, J.A.C., 1992, Landscape geochemistry—Retrospect and prospect—1990: Applied Geochemistry, v. 7, p. 1-53.

Gold, D.P., Doden, A.G., Altamura, R.J., and Sicree, A., 2005, The nature and significance of sulfide mineralization in Bald Eagle ridge at Skytop, near State College, Pennsylvania: Geological Society of America Abstracts with Programs, v. 37, no.1, p. 64.

Gould, W.D. and Kapoor, A., 2003, The microbiology of acid mine drainage, *in* Jambor, J.L., Blowes, D.W., and Ritchie, A.I.M., eds., Environmental aspects of mine wastes: Mineralogical Association of Canada Short Course Series, v. 31, p. 203-226.

Hageman, P.L., and Briggs, P.H., 2000, A simple field leach test for rapid screening and qualitative characterization of mine waste dump material on abandoned mine lands: ICARD 2000, Proceedings from the Fifth International Conference on Acid Rock Drainage, v. II, p. 1463-1475.

Hammarstrom, J.M., Piatak, N.M., Seal, R.R., II, Briggs, P.H., Meier, A.L., and Muzik, T.M., 2003a, Geochemical characteristics of TP3 mine wastes at the Elizabeth copper mine Superfund site, Orange Co., Vermont: U.S. Geological Survey Open-File Report 03-341, 40 p.

Hammarstrom, J.M., Seal, R.R., II, Meier, A.L., and Jackson, J.C., 2003b, Weathering of sulfidic shale and copper mine waste—secondary minerals and metal cycling in Great Smoky Mountains National Park, Tennessee and North Carolina, USA: Environmental Geology v. 45, p. 35-57.

Hammarstrom, J.M., Seal, R.R., II, Meier, A.L., and Kornfeld, J.M., 2004, Secondary sulfate minerals associated with acid drainage in the eastern US: recycling of metals and acidity in surficial environments: Chemical Geology, v. 215, p. 407-431.

Howe, S.S., 1981, Mineralogy, fluid inclusions, and stable isotopes of lead-zinc occurrences in central Pennsylvania: The Pennsylvania State University, unpublished M.S. thesis, 155 p.

Howe, S.S., 1988, Locations and descriptions of mineralized rock samples from Mississippi Valley-type lead-zinc occurrences in central Pennsylvania: U.S. Geological Survey Open-File Report 88-250. 37 p.

Howe, S.S., Ohmoto, H., and Rose, A.W., 1979, Sulfur isotopes of lead-zinc occurrences in central Pennsylvania: Geological Society of America Abstracts with Programs, v. 11, no. 1, p. 16-17.

Hsu, Fu-Tzu, 1973, Geochemical exploration in the Nittany Valley area, Centre County, Pennsylvania: Unpublished M. Sc. Thesis, The Pennsylvania State University, University Park, PA, 108 p.

ICDD, 2002, Powder Diffraction File Release 2002, PDF-2: International Centre for Diffraction Data, Newton Square, PA. Available from: www.icdd.com

Illsley, C. T., 1955, An investigation of geochemical prospecting by testing stream waters: Unpublished M. Sc. Thesis, The Pennsylvania State University, University Park, PA, 71 p.

Jambor, J.L.., 2003, Mine-waste mineralogy , *in* Jambor, J.L., Blowes, D.W., and Ritchie, A.I.M., eds., Environmental aspects of mine wastes: Mineralogical Association of Canada Short Course Series, v. 31, p. 117-145.

Joseph, M., 2005, State has plan for I-99 cleanup: Centre Daily Times [State College, PA], January 14, 2005 , available online at http://www.centredaily.com (Accessed 1/18/05).

Joseph, M., 2004a, Pyrite and I-99: Centre Daily Times [State College, PA], Published December 19, 2004, p. 11A .

Joseph, M., 2004b, Water worries residents: Centre Daily Times [State College, PA] , Published December 19, 2004, p. 1A .

Joseph, M., 2004c, Skytop pollution levels steady: Centre Daily Times [State College, PA], Published December 10, 2004, p. 5A.

Joseph, M., 2004d, State nears decisions on cleanup at Skytop: Centre Daily Times [State College, PA], Published November 21, 2004, p. 1A.

Joseph, M., 2004e, More pyrite unearthed at work site; Another million cubic yards of rock near Skytop being examined: Centre Daily Times [State College, PA], Published October 10, 2004, p. 1A.

Krohn, M.D., 1979, Field relations of lineaments to gossans and geochemical anomalies along Bald Eagle Mountain, Centre County, Pennsylvania: Proceedings of the International Conference on Basement Tectonics, no, 2, p. 485.

Lenker, E.S., 1962, A trace element study of selected sulfide minerals from the eastern United States: The Pennsylvania State University Ph. D. Thesis, 151 p.

Martin, J-M., and Whitfield, M., 1983, The significance of the river input of chemical elements to the ocean, *in* Wong, C.S., Boyle, E., Bruland, K.W. Burton, J.D., and Goldberg, E.D., eds., Trace metals in sea water: Plenum Press, New York, p. 265-296.

Miles, C.E., Whitfield, T.G., and others, 2001, Digital data set for the Bedrock geology of Pennsylvania: Accessed 4/4/05 at: http://www.dcnr.state.pa.us/topogeo/gismaps/digital.aspx

Miller, B.L., 1924, Lead and zinc ores of Pennsylvania: Pennsylvania Geological Survey 4th ser., Mineral Resource Report 5, 91p.

Nickelsen, R.P., Engelder, T., and McConaughy, D., 1989, Structures of the Appalachian foreland fold-thrust belt—Fold-thrust geometries of the Juniata culmination (State College and environs), Central Appalachians of Pennsylvania: Accessed 3/15/05 at: http://64.233.161.104/search?q=cache:Gahcnodzl0oJ:www.geosc.psu.edu/~engelder/geosc465/Trip.rtf+Fold-thrust+geometries+of+the+juniata&hl=en

Nordstrom, D. K., 1977, Thermochemical redox equilibria of Zobell's solution: Geochimica et Cosmochimica Acta, v. 41, p. 1835-1841.

Nordstrom, D.K., 2000, Advances in the hydrochemistry and microbiology of acid mine waters: International Geology Review, v. 42, p. 499-515.

Nordstrom, D.K., and Alpers, C.N., 1999, Geochemistry of acid mine waters, *in* Plumlee, G.S., and Logsdon, M.J., eds., The environmental geochemistry of mineral deposits, Part A.: Processes, techniques, and health issues: Society of Economic Geologists, Inc., Reviews in Economic Geology, vol. 6A, p. 133-160.

Orndorff, Z.W., 2001, Evaluation of sulfidic materials in Virginia highway corridors: Ph. D. Dissertation, Virginia Polytechnic Institute and State University, Blacksburg, VA, 175 p. Accessed 1/21/05 at: http://scholar.lib.vt.edu/theses/available/etd-10042001-123731/unrestricted/dissertation.pdf

Pennsylvania Department of Transportation (PennDOT), 2005, PennDOT District 2: Accessed 3/15/05 at: http://www.dot.state.pa.us

Perry, E., Holland, L., Evans, R., Schueck, J., and Maxwell, D., 1998, Special handling techniques in the prevention of acid mine drainage, in Pennsylvania Department of Environmental Protection, Coal mine drainage prediction and pollution prevention in Pennsylvania: Chapter 14. Accessed 1/24/05 at: http://www.dep.state.pa.us/dep/deputate/minres/districts/CMDP/main.htm

Piatak, N.M., Hammarstrom, J.M., Seal, R.R., II, Briggs, P.H., Meier, A.L., Muzik, T.L., and Jackson, J.C., 2004, Geochemical characterization of mine waste of the Ely copper mine Superfund site, Orange County, Vermont: U.S. Geological Survey Open-File Report 2004-1248, 56 p.

Plumlee, G.S., 1999, The environmental geology of mineral deposits, *in* Plumlee, G.S., and Logsdon, M.J., eds., The environmental geochemistry of mineral deposits, Part A.: Processes, techniques, and health issues: Society of Economic Geologists, Inc., Reviews in Economic Geology, vol. 6A, p. 71-116.

Plumlee, G.S., Smith, K.S., Montour, M.R., Ficklin, W.H., and Mosier, E.L. , 1999, Geologic controls on the composition of natural waters and mine waters, *in* Filipek, L.H., and Plumlee, G.S., eds., The environmental geochemistry of mineral deposits, Part B.: Case studies and research topics: Society of Economic Geologists, Inc., Reviews in Economic Geology, vol. 6B, p. 373-432.

Rimstidt, J.D. and Vaughan, D.J., 2003, Pyrite oxidation—A state-of-the-art assessment of the reaction mechanism: Geochimica et Cosmochimica Acta, v. 67, no. 5, p. 873-880.

Rose, A.W., 1999, Metallic mineral deposits—zinc-lead-silver, in Schultz, C.H., ed., The geology of Pennsylvania: Pennsylvania Geological Survey 4th ser., Special Publication 1, p. 582-587 (Co-published with the Pittsburgh Geological Society].

Schaeffer, M.F., and Clawson, P.A., 1996, Identification and treatment of potential acid-producing rocks and water quality monitoring along a transmission line in the Blue Ridge Province, southwestern North Carolina: Environmental and Engineering Geoscience v. 2, p. 35-48.

Seal, R.R., II, Johnson, A.N., Hammarstrom, J.M., and Meier, A.L., 2002, Geochemical characterization of drainage prior to reclamation at the abandoned Valzinco mine, Spotsylvania County, Virginia: U.S. Geological Survey Open-File Report 02-360, 36 p.

Shacklette, H.T., and Boerngen, J.G., 1984, Element concentrations in soils and other surficial materials of the conterminous United States: U.S. Geological Survey Professional Paper 1270, 105 p.

Sicree, A.A., 2005, Morphology and paragenesis of sulfide mineralization at Skytop on Bald Eagle ridge, Centre Co., Pennsylvania: Geological Society of America Abstracts with Programs, v. 37, no. 1, p. 64.

Singer, P.C. and Stumm, W., 1970, Acidic mine drainage—the rate determining step: Science, v.167, p. 1121-1123.

Skelly and Loy, Inc., 2004, Remediation plan I-99 construction sections A12 and C12 acid rock drainage: Report prepared for the Pennsylvania Department of Transportation, May, 2004, 51 p. Accessed 4/4/05 at: ftp://ftp.dot.state.pa.us/public/Districts/District2/i99info/REMEDIATION%20PLAN.pdf

Smith, R.C., II, 2003, Zinc and lead in central Pennsylvania, in Way, J.H., and others, eds., Geology on the edge—selected geology of Bedford, Blair, Cambria, and Somerset Counties: Guidebook, 68th Annual Field Conference of Pennsylvania Geologists, Altoona, PA, p. 63-72.

Smith, R.C., II, 1977, Zinc and lead occurrences in Pennsylvania: Pennsylvania Geological Survey Mineral Resource Report 72, 318 p.

Sobeck, R.G., Jr., 2000, Mineral mine reclamation in Knights Branch, Spotsylvania County, Virginia (Project Design Concepts): Unpublished Report, Virginia Department of Mines, Minerals, and Energy, Division of Mineral Mining, Charlottesville, Virginia, 51 p.

Sobek, A.A., Schuller, W.A., Freeman, J.R., and Smith, R.M., 1978, Field and laboratory methods applicable to overburden and minesoils: EPA 600/2-78-054, 203 p.

Southern Appalachian Forest Coalition, 2003, North Shore Road Workshops:

Taggart, J.E., Jr., 2002, Analytical methods for chemical analysis of geologic and other materials, U.S. Geological Survey: U.S. Geological Survey Open-File Report 02-0223.

Tingle, A.R., 1995, A geochemical assessment of highway construction through sulfidic rocks: M.S. Thesis, The University of Tennessee, Knoxville, 205 p.

Trumpf, W.F., Morgan, E.L., and Herrmann, R., 1979, Man induced acid drainage impact on benthic macroinvertebrate communities in the Great Smoky Mountains National Park, *in* Li, R.L., ed., Conference on Scientific Research in the National Parks, Vol. I. :National Park Service Transactions and Proceedings Series 5, p. 643-647.

U.S. EPA, 1994, Acid mine drainage prediction: Technical Document EPA530-R-94-036, 48 p. Accessed 1/21/05 at: http://www.epa.gov/epaoswer/other/mining/techdocs/amd.pdf

U.S. EPA, 2002, National recommended water quality criteria standards: EPA-822-R-02-047, Accessed March 10, 2005 at: http://epa.gov/waterscience/standards/wqcriteria.html

U.S. EPA, 2004, Preliminary remediation goals—What's new in 2004, Region 9: Superfund, PRG Table and PRG Users Guide: Accessed March 10, 2005 at: http://www.epa.gov/region09/waste/sfund/prg/index.htm

U.S. Geological Survey, 1997 to present, National field manual for the collection of water- quality data: U.S. Geological Survey Techniques of Water-Resources Investigations, Book 9, Handbooks for Water-Quality Investigations, variously paged (http://water.usgs.gov/owq/FieldManual).

Wood, C.R., 1980, Summary groundwater resources of Centre County, Pennsylvania: Pennsylvania Geological Survey, 4th Series, Water Resources Report 48, 60 p.

Yu, J.-Y., Heo, B., Choi, I.-K., Cho, J.-P., and Change, H.-W., 1999, Apparent solubilities of schwertmannite and ferrihydrite in natural stream waters polluted by mine drainage: Geochimica et Cosmochimica Acta, v. 63, p. 3407-3416.

Zentilli, M. and Fox, D., 1997, Foreword - Geology and mineralogy of the Meguma Group and their importance to environmental problems in Nova Scotia: Atlantic Geology, v.33, no. 2, p. 81-85.

Appendix A

Analytical methods for rock analyses

Gold

Summary:

Gold is determined in geological materials by DCP or atomic absorption spectrophotometry after collection by fire assay. An assay fusion consists of heating a mixture of the finely pulverized sample with about three parts of a flux until the product is molten. One of the ingredients of the flux is a lead compound which is reduced by other constituents of the flux or sample to metallic lead. The latter collects all the gold, together with silver, platinum metals, and small quantities of certain base metals present in the sample and falls to the bottom of the crucible to form a lead button. The gangue of the ore is converted by the flux into a slag sufficiently fluid so that all particles of lead may fall readily through the molten mass. The choice of a suitable flux depends on the character of the ore. The lead button is cupelled to oxidize the lead leaving behind a dore bead containing the precious metals. The dore bead is then transferred to a test tube, dissolved with aqua regia, diluted to a specific volume and determined by DCP or atomic absorption spectrophotometry.

The lower reporting level for a 15 g sample charge is 5 ppb by DCP and atomic absorption.

The upper reporting limit is 10,000 ppb.

Sample weight: 15 g

Analytical Performance

Data will be deemed acceptable if recovery of gold is ±20% at five times the LOD and the calculated percent RSD of duplicate samples is no greater than 20%.

Total Sulfur

Summary:

Total sulfur is determined by using an automated sulfur analyzer. Approximately 0.25 g of sample is mixed with iron chips and LECOCEL and is heated in a combustion tube in a stream of oxygen at high temperature. Sulfur is oxidized to sulfur dioxide. Moisture and dust are removed and the sulfur dioxide gas is then measured by a CS-244 infrared detector.

The reporting range for total sulfur is from 0.05% to about 35%.

Sample weight: 0.25 g

Analytical Performance

Data will be deemed acceptable if recovery of total sulfur is ±15% at five times the LOD and the calculated percent RSD of duplicate samples is no greater than 15%.

Total Carbon

Summary:

Total carbon in geologic materials is determined by the use of an automated carbon analyzer. A weighed sample is combusted in an oxygen atmosphere at 1370°C to oxidize carbon to carbon dioxide. Moisture and dust are removed and the carbon dioxide gas is measured by a solid state infrared detector.

The operating range for total carbon is from 0.05% to about 30%.

Sample weight: 0.25 g

Analytical Performance

Data will be deemed acceptable if recovery of total carbon is ±15% at five times the LOD and the calculated percent RSD of duplicate samples is no greater the 15%.

Carbonate Carbon

Summary:

Carbonate carbon in geologic materials is determined as carbon dioxide by coulometric titration. The sample is treated with hot 2N perchloric acid and the evolved carbon dioxide is passed into a cell containing a solution of monoethanolamine. The carbon dioxide, quantitatively absorbed by the monoethanolamine, is coulometrically titrated using platinum and silver/potassium-iodide electrodes. The lower reporting limit is 0.01% carbon dioxide and samples containing up to 50% carbon dioxide may be analyzed. Sample size is adjusted from 0.5 f for the range 0.01 to 5% carbon dioxide, 0.1 g for the range 5 to 10% carbon dioxide, and 0.02 g for greater than 10% carbon dioxide.

Sample weight: up to 0.1 g

Analytical Performance

Data will be deemed acceptable if recovery for carbonate carbon is ±15% at five times the lower limit of determination and the calculated percent RSD of duplicate samples is no greater than 15%.

42 Element ICP-AES-MS multi-acid, total

Summary:

Forty-two major, minor, and trace elements are determined in geological materials by inductively coupled plasma-atomic emission spectrometry (ICP-AES) and inductively coupled plasma-mass spectrometry (ICP-MS). The sample is decomposed using a mixture of hydrochloric, nitric, perchloric, and hydrofluoric acids at low temperature. An aliquot of the digested sample is aspirated into the ICP-AES and the ICP-MS. The concentrations of the optimal elements from the ICPAES and ICPMS are determined. Calibration on the ICPAES is performed by standardizing with digested rock reference materials and a series of multi-element solution standards. The ICPMS is calibrated with aqueous standards, and internal standards are used to compensate for matrix affects and internal drifts.

Sample weight: 0.25 g

Reporting limits for 42 elements by ICP-AES-MS:

Element	Concentration Range	
Aluminum, Al	0.01%	15%
Calcium, Ca	0.01%	15%
Iron, Fe	0.01%	15%
Potassium, K	0.01%	15%
Magnesium, Mg	0.01%	15%
Sodium, Na	0.01%	15%
Phosphorous, P	50 ppm	1%
Titanium, Ti	0.01%	15%
Silver, Ag	1 ppm	10 ppm
Arsenic, As	1 ppm	1%
Barium, Ba	5 ppm	1%
Beryllium, Be	0.1 ppm	100 ppm
Bismuth, Bi	0.04 ppm	1%
Cadmium, Cd	0.1 ppm	1%
Cerium, Ce	0.05 ppm	0.1%
Cobalt, Co	0.1 ppm	1%
Chromium, Cr	1 ppm	1%
Cesium, Cs	0.05 ppm	0.1%
Copper, Cu	0.5 ppm	1%
Gallium, Ga	0.05 ppm	500 ppm
Indium, In	0.02 ppm	0.05%
Lanthanum, La	0.5 ppm	0.1%
Lithium, Li	1 ppm	5%
Manganese, Mn	5 ppm	1%
Molybdenum, Mo	0.05 ppm	1%
Niobium, Nb	0.1 ppm	0.1%
Nickel, Ni	0.5 ppm	1%
Lead, Pb	0.5 ppm	1%
Rubidium, Rb	0.2 ppm	1%
Sulfur, S	0.01 %	5%
Antimony, Sb	0.05 ppm	1%

Scandium, Sc	0.1 ppm	0.1%
Tin, Sn	0.1 ppm	0.1%
Strontium, Sr	0.5 ppm	1%
Tellurium, Te	0.1 ppm	0.05%
Thallium, Tl	0.1 ppm	1%
Thorium, Th	0.2 ppm	1%
Uranium, U	0.1 ppm	1%
Vanadium, V	1 ppm	1%
Tungsten, W	0.1 ppm	1%
Yttrium, Y	0.1 ppm	1%
Zinc, Zn	1 ppm	1%

Analytical Performance

Data is deemed acceptable if recovery for all 42 elements is ±15% at five times the Lower Limit of Determination (LOD) and the calculated Relative Standard Deviation (RSD) of duplicate samples is no greater than 15%.

Appendix B

Leachate chemistry for Skytop soil composite

Latitude	40.83310
Longitude	-77.96722
Collection Date	6/14/04
Leach date	1/5/05
Leachate pH	4.20
pH	4.067
Temperature (oC)	22
Dissolved O_2 (mg/L)	8
ORP raw	303.10
ORPstandard	203.4@21.4
ORP corrected (mV)	521.37
Specific conductance (µS/cm)	1595
Fe^{2+} (mg/L) Hach	10.90
Fe total (mg/L) Hach	10.90

Element	Units	Method	
		Anions	
Cl	ppm	IC	12.5
F	ppm	IC	5.7
NO_3	ppm	IC	2.2
SO_4	ppm	IC	1,657
		Cations	
Ag	µg/L	ICP-AES	<10
Ag	µg/L	ICP-MS	<3
Al	µg/L	ICP-AES	24,800
Al	µg/L	ICP-MS	22,900
As	µg/L	ICP-AES	<100
As	µg/L	ICP-MS	<1
B	µg/L	ICP-AES	<20
Ba	µg/L	ICP-AES	12.5
Ba	µg/L	ICP-MS	12.4
Be	µg/L	ICP-AES	<5
Be	µg/L	ICP-MS	1.4
Bi	µg/L	ICP-MS	< 0.2
Ca	µg/L	ICP-AES	376
Ca	µg/L	ICP-MS	368
Cd	µg/L	ICP-AES	33.4
Cd	µg/L	ICP-MS	34.2
Ce	µg/L	ICP-MS	10.8

Element	Units	Method	
Co	µg/L	ICP-AES	186
Co	µg/L	ICP-MS	170
Cr	µg/L	ICP-AES	<10
Cr	µg/L	ICP-MS	1
Cs	µg/L	ICP-MS	< 0.02
Cu	µg/L	ICP-AES	439
Cu	µg/L	ICP-MS	397
Dy	µg/L	ICP-MS	7.71
Er	µg/L	ICP-MS	5.14
Eu	µg/L	ICP-MS	1.34
Fe	µg/L	ICP-AES	11,000
Fe	µg/L	ICP-MS	11,600
Ga	µg/L	ICP-MS	0.07
Gd	µg/L	ICP-MS	6.67
Ge	µg/L	ICP-MS	0.33
Ho	µg/L	ICP-MS	1.77
K	µg/L	ICP-AES	<0.1
K	µg/L	ICP-MS	0.07
La	µg/L	ICP-MS	3.72
Li	µg/L	ICP-AES	12.5
Li	µg/L	ICP-MS	9.8
Lu	µg/L	ICP-MS	0.6
Mg	µg/L	ICP-AES	6.15
Mg	µg/L	ICP-MS	5.44
Mn	µg/L	ICP-AES	172
Mn	µg/L	ICP-MS	166
Mo	µg/L	ICP-AES	<20
Mo	µg/L	ICP-MS	< 2
Na	µg/L	ICP-AES	<0.1
Na	µg/L	ICP-MS	<0.5
Nb	µg/L	ICP-MS	< 0.2
Nd	µg/L	ICP-MS	11
Ni	µg/L	ICP-AES	332
Ni	µg/L	ICP-MS	326
P	µg/L	ICP-AES	<0.1
P	µg/L	ICP-MS	< 0.01
Pb	µg/L	ICP-AES	<100
Pb	µg/L	ICP-MS	0.2
Pr	µg/L	ICP-MS	1.77
Rb	µg/L	ICP-MS	0.32
Sb	µg/L	ICP-AES	<100
Sb	µg/L	ICP-MS	<0.3
Sc	µg/L	ICP-MS	5.1
Se	µg/L	ICP-MS	< 1
SiO2	µg/L	ICP-AES	1.31
SiO2	µg/L	ICP-MS	1.3
Sm	µg/L	ICP-MS	5.03
SO4	µg/L	ICP-MS	1,080
Sr	µg/L	ICP-AES	353
Sr	µg/L	ICP-MS	337
Ta	µg/L	ICP-MS	< 0.02
Tb	µg/L	ICP-MS	1.18

Element	Units	Method	
Th	µg/L	ICP-MS	< 0.2
Ti	µg/L	ICP-AES	<50
Ti	µg/L	ICP-MS	24
Tl	µg/L	ICP-MS	<0.1
Tm	µg/L	ICP-MS	0.77
U	µg/L	ICP-MS	6.14
V	µg/L	ICP-AES	<10
V	µg/L	ICP-MS	<0.5
W	µg/L	ICP-MS	< 0.5
Y	µg/L	ICP-MS	39.7
Yb	µg/L	ICP-MS	4.43
Zn	µg/L	ICP-AES	9,810
Zn	µg/L	ICP-MS	9,580
Zr	µg/L	ICP-MS	< 0.2